Regenerated Fibre Bragg Gratings

Citation for published version:
Polz, L, Dutz, FJ, Maier, RRJ, Bartelt, H & Roths, J 2021, 'Regenerated Fibre Bragg Gratings: A Critical Assessment of more than 20 Years of Investigations', *Optics and Laser Technology*, vol. 134, 106650. https://doi.org/10.1016/j.optlastec.2020.106650

Digital Object Identifier (DOI):
10.1016/j.optlastec.2020.106650

Link:
Link to publication record in Heriot-Watt Research Portal

Document Version:
Peer reviewed version

Published In:
Optics and Laser Technology

Article

Regenerated Fibre Bragg Gratings: A Critical Assessment of more than 20 Years of Investigations

Leonhard Polz [a,d], Franz Dutz [d], Robert R.J. Maier [b], Hartmut Bartelt [c], Johannes Roths [d]

[a] OHB System AG, Manfred-Fuchs-Str. 1, 82234 Wessling, Germany
[b] Heriot-Watt University, School of Engineering and Physical Sciences, Riccarton Campus, Edinburgh, EH14 4AS, United Kingdom
[c] Leibniz Institute of Photonic Technology, Albert-Einstein-Str. 9, 07745 Jena, Germany
[d] Munich University of Applied Sciences, Photonics Laboratory, Lothstr. 39, 80335 Munich, Germany

HIGHLIGHTS

- Regenerated Fibre Bragg Gratings (RFBG) and Chemical Composition Gratings (CCG)
- An up to date examination of the research status on RFBG and CCG
- Crystallization theory, chemical composition theory and negative index theory are discussed
- Key parameters for RFBG / CCG production are reviewed
- An overview of actual and future RFBG / CCG applications is given

ARTICLE INFO
Keywords:
Fibre Bragg Grating
Regenerated grating
Chemical composition grating
High temperature sensing
Nano-crystalline FBG
Negative index grating

ABSTRACT

Regenerated fibre Bragg gratings are formed when specially pre-treated seed gratings are heated up to several hundred degrees centigrade. During this process, the fibre Bragg grating (FBG) reflectivity vanishes and regrows, forming a regenerated grating, which can survive temperatures of more than 1000 °C. Right from the beginning, it was clear that the extraordinary temperature stability of regenerated FBGs will open new fields of applications for FBGs. Multiple investigations have been made to explore the mechanisms of the regeneration effect, often presenting contradictory explanations of the processes leading to their formation. To date, there is no comprehensive theory which can explain all the observed phenomena regarding the regeneration effect. However, a broad base of knowledge exists, which can be used for tailored manufacturing and application of regenerated FBG. In this article, we present a summary of the breadth of regenerated FBG research, including a critical overview and discussion of the various competing theories published to date. We conclude with an outlook on present and future applications of regenerated FBGs and identify further research necessary to unambiguously identify and explain the key processes occurring during regeneration.

1. Introduction

Fibre Bragg gratings (FBG) are used as in-fibre solutions for fibre optic filters, reflectors or sensors [1-3]. The first FBG was developed in 1979 by creating a 488 nm standing wave inside a Ge-doped fibre [4]. Interferometric side illumination techniques [5] as well as mask illumination methods [6] further enabled the ability to choose period and bandwidth of the gratings independently. Today, multiple possibilities exist to create different kinds of FBGs, which differ not only in their production process but also in their performance and spectral characteristics [7]. Some of these types of FBGs, including regenerated FBGs (RFBGs), feature a higher temperature stability than commonly used gratings [8], which is of great interest for industries such as oil and gas, aerospace, the energy sector, process monitoring as well as for high power lasers.

The most commonly used type I FBGs exhibit a decrease in reflectivity over time when heated to temperatures of a few hundred degrees centigrade, until their reflectivity has completely vanished [9] (more details on type I, type II and type IIA gratings, which are also mentioned in this paper will be found in section 2). All the above listed gratings are made in a single step manufacturing process, whereas RFBGs, in contrast, are made from a seed grating which is subjected to a specific annealing process, during which the reflectivity of the grating at first vanishes after a certain time at high temperatures, but is then re-growing and stabilising, as can be seen in Figure 1 (Graph adapted from [10]). Here, a seed grating in SMF28 fibre was annealed for 100 h at a constant temperature of 800 °C. The seed grating decayed and vanished after 6 h, but directly afterwards the regenerated grating started to grow and achieved a stable reflectivity. The fact that regeneration can happen at constant temperatures demonstrates that the refractive index increase during regeneration is not related to any temperature changes, but there is a time dependent physical or chemical process going on inside the fibre.

Because of this vanishing and re-growing characteristic of the grating signal the term "regeneration" has been adopted, and the temperature at which this happens has been called the regeneration temperature. As a general guide, typical regeneration temperatures are in the order of 500 °C to 900 °C for the majority of reported RFBGs manufactured in Ge and F doped fused silica fibres. However, in some extreme cases regeneration temperatures of up to 1200 °C have been reported, depending on glass composition and the duration of exposure to the regeneration heat source [11]. In addition to the notation of "regenerated grating", other terms such as "chemical composition grating" (CCG) [12], "tetrahedral FBG" (TFBG) [13], or "nano-crystalline FBG" (NFBG) [14] are used in published literature, for gratings which are fabricated in this two-stage process. This multitude of terms is, in some way a reflection of the sometimes conflicting theories and assumptions made to explain the regeneration process. Regardless of whatever they are called, the main features of RFBGs are their increased temperature stability and the decay of the reflectivity (mostly down to zero) and its regrowth with time during a continued annealing at high temperatures.

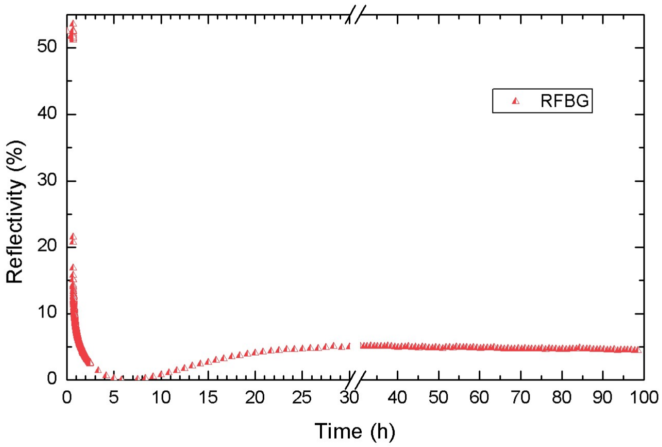

Figure 1: Typical evolution of a grating's reflectivity during regeneration showing the near complete loss of reflectivity after 6 h at a constant temperature of 800 °C and the subsequent recovery of reflectivity. (Graph adapted from [10])

Another type of high temperature stable FBGs are type II FBGs, often produced with fs-laser irradiation [15]. RFBGs and type II FBGs show very similar temperature stability in reflectivity, but both types of gratings need to undergo an annealing process to show a good wavelength stability at high temperatures [10]. Especially for point-by-point written type II FBGs, strong cladding mode coupling was reported, which can limit its multiplexing capability [16]. RFBGs, in contrast, show impeccable multiplexing capabilities (compare also section 5).

Before focussing on the different investigations on RFBGs, some important basics about FBGs in general and more information about different types of FBG are recapitulated in section 2. In section 3 the initial studies regarding RFBG and the relevant theories, which were developed to explain their physical background, are presented and discussed. Although there are, to date, no comprehensive and broadly accepted explanations for the processes taking place during annealing and regeneration, it is possible to summarize some key factors affecting the formation of RFBGs, which are described in section 4. Section 5 presents selected applications of RFBGs and is followed by an overall conclusion.

2. Fibre Bragg grating basics

In this section, we present only a brief extract of FBG types and the most fundamental aspects and parameters of FBG theory, relevant to the discussions in this paper. The detailed theory is presented in numerous text books [17, 18]. A more comprehensive list about the existing types of FBG can be found in [7].

2.1. FBG spectral reflection

An FBG consists of a periodic variation of the refractive index in the core of an optical fibre along its axis z over the length L, as shown in Figure 2. For the simple case of a uniform grating, the refractive index distribution over the length L can be written as

$$n_{FBG}(\mathrm{z}) = n_{eff} + \Delta n_{DC,eff} + \Delta n_{AC,eff} \cdot \sin\left(\frac{2\pi\cdot \mathrm{z}}{\Lambda_{FBG}}\right). \quad (1)$$

Here n_{eff} is the effective refractive index of the pristine fibre, which has values between n_{core} and $n_{cladding}$; $\Delta n_{DC,eff}$ is the change of the mean value over L of the effective refractive index due to the grating inscription; $\Delta n_{AC,eff}$ describes the strength of the modulation of the refractive index, and Λ_{FBG} is the period of the grating. The Bragg wavelength, λ_B, which is the central wavelength of the reflected spectra, is given by

$$\lambda_B = 2\left(n_{eff} + \Delta n_{DC,eff}\right) \cdot \Lambda_{FBG}. \quad (2)$$

Using the coupled mode theory [17, 18], the spectral reflectivity $R(\lambda)$ of a uniform grating can be derived,

$$R(\lambda) = \frac{\sinh^2\left(\sqrt{\kappa^2-\hat{\sigma}^2}\cdot L\right)}{\cosh^2\left(\sqrt{\kappa^2-\hat{\sigma}^2}\cdot L\right)-\frac{\hat{\sigma}^2}{\kappa^2}}, \quad (3)$$

containing the wavelength dependent coupling coefficients $\hat{\sigma}$ and κ [18]. The AC coupling coefficient κ describes the strength of the grating. It is determined by the amplitude of the refractive index modulation $\Delta n_{AC,eff}$ as

$$\kappa = \frac{\pi}{\lambda} \cdot \Delta n_{AC,eff} \quad (4)$$

and shows just a small wavelength dependence around λ_B.

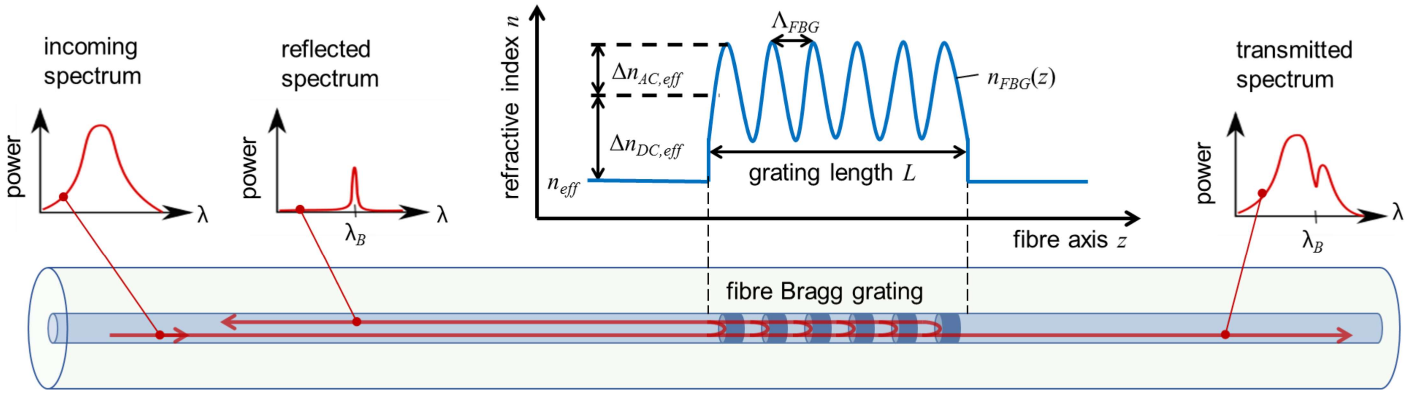

Figure 2: Fibre Bragg grating principle. If spectrally broad light waves are guided in a fibre, the fibre Bragg grating (FBG) only reflects light with wavelengths close to a particular wavelength, the so-called Bragg wavelength λ_B.

The DC self-coupling coefficient $\hat{\sigma}$ determines the central wavelength of the Bragg reflection and is defined as

$$\hat{\sigma} = 2\pi\left(n_{eff} + \Delta n_{DC,eff}\right) \cdot \left(\frac{1}{\lambda} - \frac{1}{\lambda_B}\right). \quad (5)$$

Thus, for $\lambda = \lambda_B$, $\hat{\sigma}$ becomes 0. With $\hat{\sigma} = 0$ and $\frac{\sinh}{\cosh} = \tanh$, Eq. (3) reduces to

$$R(\lambda_B) = \tanh^2(\kappa \cdot L) = \tanh^2\left(\frac{\pi \cdot L}{\lambda_B} \cdot \Delta n_{AC,eff}\right). \quad (6)$$

Using Eq. (6), the known length of the grating L, and the measured reflectivity $R(\lambda_B)$ at the maximum of the Bragg peak, the absolute value of $\Delta n_{AC,eff}$ can be calculated:

$$\pm\Delta n_{AC,eff} = \frac{\lambda_B \cdot \operatorname{atanh}\left(\sqrt{R(\lambda_B)}\right)}{\pi \cdot L}. \quad (7)$$

Since the cladding is often not photosensitive, the refractive index change is only located within the fibre core. $\Delta n_{DC,core}$ and $\Delta n_{AC,core}$ are related to the changes in effective refractive index by the power confinement factor Γ [19],

$$\Delta n_{AC,eff} = \Gamma \cdot \Delta n_{AC,core}, \quad (8)$$

$$\Delta n_{DC,eff} = \Gamma \cdot \Delta n_{DC,core}, \quad (9)$$

where Γ describes the amount of power of the mode which is guided inside the fibre core.

2.2. Type I gratings

The most widely used type of FBGs are type I gratings. They are typically inscribed using UV-Excimer lasers or frequency doubled CW-Ar ion lasers. Different optical configurations are used to create sinusoidal interference patterns, which exhibit the necessary periodicity on the nanometre scale to create the FBG [17]. The fibre is placed within this pattern and the pattern is transferred into the optical fibre by photochemical processes [20]. For simplification, in this paper the areas of constructive interference and thereby higher laser irradiation will be termed *illuminated areas*, whereas the regions of lower irradiation will be called *non-illuminated* areas. Most of the commonly used fused silica fibres contain Ge-doping in their core and during the fibre production germanium oxygen deficient centres (GODC) are formed within the glass structure [17, 18]. The most prominent GODC e.g. is the Ge-Ge "wrong bond". During FBG inscription UV light is absorbed in the illuminated areas by these GODCs and electrons are excited into the conduction band. In this way, the GODC is transferred to a GeE' defect, consisting of a single unpaired electron at the Ge atom. This GeE' defect is supposed to be one of the main contributors to the refractive index change during FBG writing. The excited electron in the conduction band is caught elsewhere in the glass structure by an electron trap. In these traps, the electrons are held until they are excited again by UV light or thermal energy. This means, that especially at higher temperatures, the electrons can be released and recombine with the GeE' defects and reverse the UV-induced refractive index change. Erdogan et al. established a model which describes this temperature-dependent decay of type I gratings [9] (A typical type I grating decay in pristine fibre with increasing temperature can be seen e.g. in Figure 3).

Annealing of a type I FBG for a period of time in the order of a few hours decreases but also stabilizes the reflectivity for a temperature range up to the annealing temperature. It was found that the reflectivity of such a "pre-annealed" type I FBG can increase with increasing temperature because of the temperature dependence of the confinement factor Γ, i.e. the fraction of power of the mode that is guided inside the core increases slightly with temperature [21]. At higher confinement of a core mode the interaction of this mode with the FBG structure in the core increases which leads to a higher reflectivity. This process is time independent and reversible with temperature and is thus distinctly different to the regeneration process of an FBG.

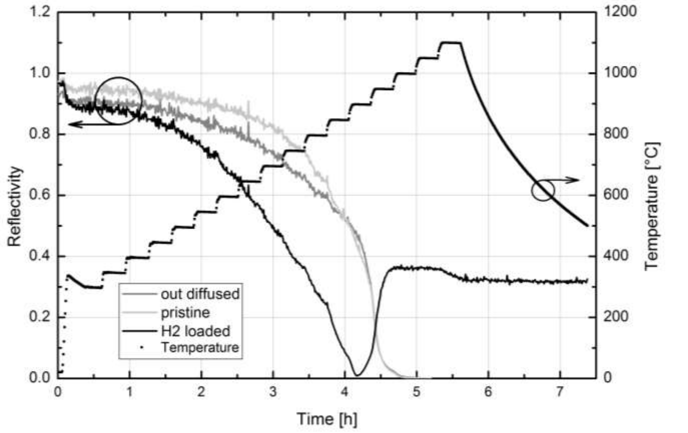

Figure 3: Degradation of the grating strength of three gratings inscribed in SMF28 fibre with different pre-treatment. Only the grating in the fibre containing H_2 during inscription regenerates. (Graph taken from [22])

2.3. RFBGs and other high temperature FBGs in silica fibres

To increase the photosensitivity of the fibre, but also to allow regeneration of the FBG, fibres can be loaded with hydrogen prior to FBG inscription. To this end, the fibre has to be exposed to an atmosphere with very high hydrogen concentration, so that H_2 molecules diffuse into the glass structure until a concentration equilibrium inside and outside the fibre is reached [23]. This can be done by exposing the fibre to high hydrogen gas pressure [24] or by OH-flooding (flame brushing) in a hydrogen-rich flame [25]. To write FBGs in H_2 loaded fibres, the same techniques can be used as for unloaded fibres. Beside the formation of GeE' from GODC defects, here also the hydrogen molecules react with oxygen atoms in the glass structure to form hydroxyl groups, which also increase the refractive index. These reactions were verified by the observed decrease in absorption at 1240 nm (H_2) and the increase at 1390 nm (Si-OH) and 1410 nm (Ge-OH) [18]. Hydrides like Ge-H, in contrast, were observed only in small amounts [26]. Figure 3 is taken from [22] and compares the reflectivity evolution with increasing temperature of type I gratings in pristine, H_2 loaded and H_2 loaded but out diffused fibres. For the trace "H2 loaded" fibres were loaded with hydrogen under high pressure prior to the grating inscription and H_2 is still present when the UV-inscription of the FBG takes place, whereas in the out-diffused fibre all hydrogen previously loaded in a similar high pressure process has left the fibre. The gratings in the pristine and out-diffused fibres decrease and vanish with temperature and they do not regrow or regenerate. In contrast, the reflectivity of the seed grating in the fibre containing H_2 during inscription decreases much faster but after vanishing it regrows, thus forming an RFBG. The temperature at which the seed grating disappears and the RFBG starts growing is called *regeneration temperature*.

Another possibility to create an FBG is to create pores or micro cavities inside the fibre core as it is done for type II or type IIA gratings [7, 20, 27]. These pores or cavities cause a decrease of the refractive index in the illuminated areas and therefore the gratings are also called *negative index gratings*. Since these gratings are based on volume damages in the glass structure, instead of single broken bonds, they are more temperature stable than type I gratings. Type II gratings show similar temperature stability as regenerated gratings [10, 15]. Type IIA gratings, formed in highly doped fibres using UV inscription are sometimes considered to be less temperature stable than type II gratings, because of the highly doped fibre cores. However, as the type classification indicates, there is little difference between type II and type IIA gratings. For type II gratings, the negative index change dominates right from the beginning of inscription, whereas for a type IIA grating, a significant positive index change is produced as well, at the start of the FBG inscription. This is shown in Figure 4 which plots the typical evolution of reflectivity and Bragg wavelength during inscription of a type IIA grating. At the start of the inscription process, there is mainly positive index change (type I part). After a certain amount of cumulated fluence, thermal induced stress and densification exceed the threshold stress level and the negative index pore formation begins (type II part) [28]. From this point, the reflectivity starts to decrease, until it reaches almost zero, when positive and negative index contributions have the same strength. With further illumination, the type II part starts to exceed the type I part and the reflectivity increases again. When pore and micro cavity formation starts, the Bragg wavelength stops growing and can even decrease with increasing cumulative fluence. This means, the influence of type I and type II index change on $\Delta n_{DC,eff}$ per pulse cancel out.

During fibre drawing significant levels of stress and strain are frozen into the fibre structure, mostly due to rapid cooling but also due to the applied mechanical forces and the difference in coefficient of thermal expansion (CTE) between core and cladding [29]. Different CTE of core and cladding cause thermal stress in radial and axial direction. These stresses are primarily located at the core-cladding interface. The rapid cool down in the draw tower lead to a lower material density, especially in doped glasses, and thereby lower refractive index. Regeneration takes place at temperatures close to, or above, the respective glass transition temperature and these frozen-in stresses and strains can be healed and relieved when heating the fibre close to the glass transition temperature [30]. This will in turn cause significant changes to the effective refractive index [31].

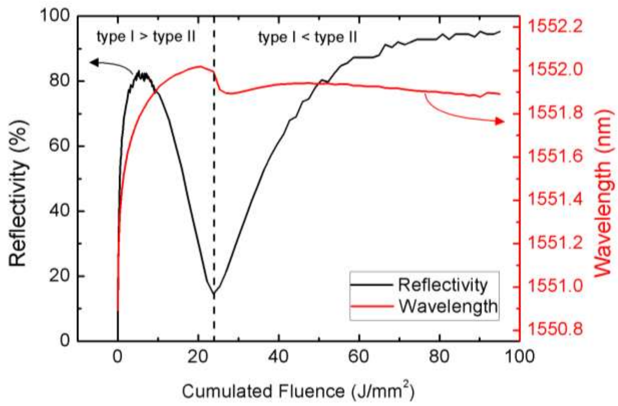

Figure 4: Typical reflectivity (black) and wavelength (red) evolution over cumulated fluence during type IIA grating inscription using a UV-laser setup described in [32] and a fibre with high GeO_2-doping (18%) in a 5 µm diameter core (IPHT, Jena).

3. Theories and studies on the mechanism leading to the formation of RFBG

3.1. First experiments with fluorine doped fibres

In 1997, Fokine et al. published the first investigation of the formation of a regenerated FBG in a hydrogen-loaded fibre [33]. The fibre used in in Fokine's paper [33] had a germanium doped fibre core but was also co-doped with fluorine. In developing a theory underpinning their observations they argued that the observed regeneration phenomenon relates to the presence of fluorine, which is removed from the fibre in the illuminated areas. When an FBG is inscribed in a hydrogen-loaded fibre, beside the GeE' defects, OH groups are generated within the illuminated areas in addition to the GeE' defects (compare section 2). These OH groups cause a removal of F-atoms out of the glass structure, when the fibre is heated to higher temperatures. The proposed reaction pathways are shown in Eq. (10) to (12) [12, 25].

$$\equiv Si - OH + F - Si \equiv \rightarrow \equiv Si - O - Si \equiv + HF. \quad (10)$$

Since the amount of OH groups and molecular H_2O is always balanced in glass, there is also the possibility of an ion exchange,

$$2 \equiv Si - OH \leftrightarrow \equiv Si - O - Si \equiv + H_2O, \quad (11)$$

$$\equiv Si - F + H_2O \equiv \rightarrow \equiv Si - OH + HF. \quad (12)$$

Reactions pathways (10) and (12) are only preferred at higher temperatures, because at lower temperatures, the reaction equilibrium of both reactions is on the Si-F side (e.g. etching of glass with HF-acid or reduction of OH absorption due to F-doping). This is possible because the equilibrium state can change with temperature. Moreover, HF molecules are highly mobile and at higher temperatures diffuse out of the core very quickly. This in turn increases the reaction rates of Eq. (10) and Eq. (12), leading to a removal of fluorine from the fibre core and was proven by time-of-flight secondary ion mass spectroscopy [34]. During FBG writing, OH groups are formed only within the illuminated areas, hence during regeneration, fluorine is removed only from these areas. Therefore, the chemical composition of the glass is changed according to the UV intensity pattern. Since F-doping reduces the refractive index of glass, this causes also a spatial modulation of the refractive index. According to this theory, the gratings are based on periodic variations of the chemical composition of the glass, which led to the naming of CCG for this type of RFBGs [12, 25, 33, 35-38].

Fokine observed that RFBGs in Ge-F co-doped fibres became strongest when heated for 24 min. at temperatures between 600 °C and 700 °C before being heated up to the regeneration temperature at 1000 °C [12]. Fokine argued that between 600 °C and 700 °C, fluorine and OH groups are already forming HF molecules, but only in the illuminated areas, because at these temperatures the OH groups are still too immobile to diffuse into the non-illuminated regions. By direct regeneration at 1000 °C, the OH groups are already diffusing so fast that HF molecules are also formed in the non-illuminated areas, which lowers the grating contrast. However, during this pre-treatment between 600 °C and 700 °C, Fokine was not able to see any increases in the reflectivity of the gratings, as one might expect from the relation between fluorine and refractive index. However, by heating the grating to 1000 °C the regeneration was observed. Fokine argued that this was because only above 1000 °C the glass structure can reach again an equilibrium state in the areas where fluorine was diffused-out and this finally changes the refractive index [36].

To erase an RFBG, according to Fokine's CCG theory, fluorine must dissociate from Si and diffuse from the non-illuminated areas to the illuminated areas in its molecular form. Since there is no hydrogen left within the fibre after the formation of the RFBG the fluorine dissociation is reduced as this requires higher activation energy. He proposed a model to describe this diffusion [25, 37] and observed that for temperatures above 1000 °C the measured decay of RFBGs fits very well to the known diffusion constants of F_2 in glass [36].

3.2. RFBG in fibres without fluorine

In the years following Fokine's first publications, it was found, that RFBGs can also be generated in fibres without F-doping [38-40]. Fokine interpreted these gratings as oxygen-CCG (O-CCG), where the concentration of oxygen is modulated along the core of the fibre [38]. According to Eq. (11), at high temperatures, two OH groups can form a water molecule that diffuses out of the fibre. In comparison to the chemical composition of the fibre core before hydrogen loading, there is now a reduced amount of oxygen in the illuminated areas in comparison to the non-illuminated areas which are the basis for the O-CCG. Similar to fluorine doped fibres, it was shown that, after regeneration, the high temperature decay rate of RFBGs in fibres without fluorine fit to the diffusion constants of O_2 in glass [36].

In 2008, Canning presented an alternative model explaining the regeneration phenomena in fibres with Ge doped cores [41], whose steps are described in Figure 5. It is known that the fibre drawing process leads to high radial tensile stress between the fibre core and the pure silica cladding (Figure 5a) due to the higher CTE of Ge doped glass [29]. There are indications in [42] that this stress can be reduced if OH groups are formed within the fibre core. OH groups are only formed in the UV illuminated areas during FBG writing in hydrogen-loaded fibres. Hence, it is conceivable that there is a periodic stress variation at the core-cladding interface for type I FBGs in hydrogen-loaded fibres (Figure 5b). If this type I FBG is heated to high temperatures, the core-cladding interface stress is released in the non-illuminated areas and compressive radial stress will occur in the illuminated areas of the FBG (Figure 5c). Compressive stress in combination with high temperatures can lead to a crystallization of the glass to cristobalite or tridymite [41, 42]. Since cristobalite and tridymite exhibit higher densities than fused silica, they show also higher refractive indices. An FBG based on localised cristobalite or tridymite crystals is also expected to be extremely temperature stable up to the melting temperature of the crystals. However, at and above the regeneration temperature these seed crystals can continuously grow into the non-illuminated areas of the FBG (Figure 5d). This will slowly decrease the refractive index contrast of the FBG and thereby reduce the reflectivity which fits the experimental observations of RFBG decays at high temperatures [38, 43-45]. Instead, the mean refractive index $\Delta n_{DC,eff}$ instead should be growing continuously.

In 2012 Canning modified his theory, since it seems to be possible to generate RFBGs also in helium loaded fibres [46]. According to Canning, this regeneration was enabled by the amorphous structure of the glass, which is inflated when the fibre is loaded with H_2 or He under high pressure [47]. The inflated structure allows mechanical rearrangements within the glass and interactions of defects and therewith the reduction of the core-cladding stress in the illuminated areas. As described before, at high temperatures this would lead to compressive stress and crystallization in these areas. However, the presented observations of RFBG in He loaded fibres in [46] are not unambiguous, since only one of the two FBGs in He loaded fibres showed regeneration. Furthermore, no other publications have been found, to date, which report regeneration after helium loading.

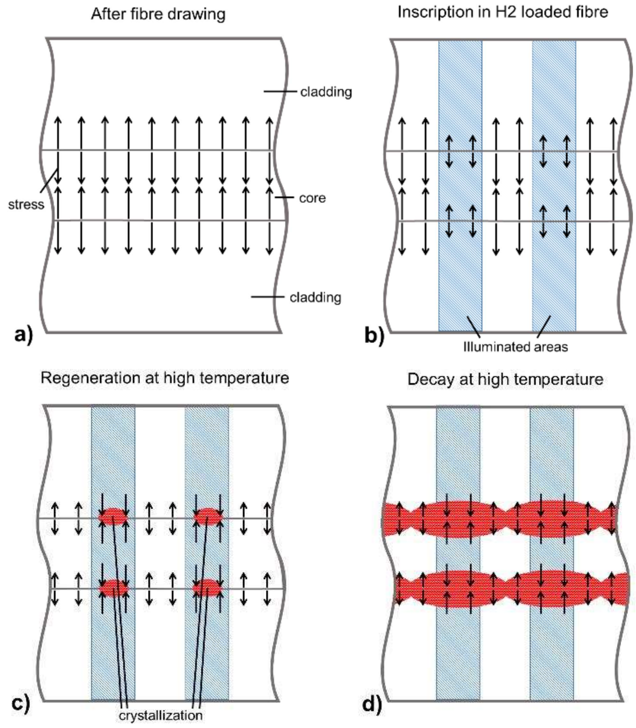

Figure 5: Crystallization theory: a) After fibre drawing, there is a radial tensile stress between fibre core and cladding because of the higher coefficient of thermal expansion (CTE) of the Ge doped core. b) During inscription of an FBG in hydrogen-loaded fibre, the stress at the core-cladding interface is reduced in the illuminated areas due to the formation of OH. c) With increasing temperatures the tensile core-cladding interface stress reduces and can even invert to compressive stress in the illuminated areas. This can lead to crystallization in these areas. d) At high temperatures, the crystalline areas grow into the non-illuminated areas and the contrast of the refractive index modulation is reduced in the RFBG.

Table 1: Main characteristics of crystallization and chemical composition theory

Theory	Crystallization	Chemical composition
Physical effect	Cristobalite or tridymite formation	Modulation of oxygen or fluorine concentration
Pre-conditions necessary during/after seed grating inscription	Reduction of core-cladding stress due to OH formation or hydrogen/helium diffusion	OH formation
Expected $\Delta n_{DC,eff}$ during regeneration	Increase	Increase
Expected $\Delta n_{DC,eff}$ during RFBG decay	Increase	Stable

The main characteristics of both theories are summarized in Table 1. The crystallization theory of Canning is supported by the observation that regeneration can be affected by applying longitudinal tension in the fibre [48, 49]. Due to the tension, the stress conditions at the core-cladding interface are changed, thereby changing the preconditions for the formation of seed crystals and their favoured direction of growth. If the formation of RFBGs was based on OH diffusion and chemical reactions, as argued by Fokine, these observations would have to be explained by a dependency of the reaction rate, reaction equilibrium or diffusion coefficient on the stress conditions within the glass, which seems to be unlikely. Conversely, over the past few years, there have also been observations which were inconsistent with Canning's theory. Measurements of stress conditions within fibres do not show any significant change due to H_2 loading [50]. Moreover, Yang et al. succeeded in regenerating seed FBGs in fibres where the cladding was completely etched away before regeneration [51]. Due to the missing interface between core and cladding no stress could persist, but the FBG regenerated nevertheless. However, they observed different regeneration temperatures depending on whether the cladding was etched or not. This indicates that stress within the fibre and at the core-cladding interface cannot be the sole reason of the regeneration phenomena, although it is clear that such a stress when present has an effect on regeneration process. It was also observed that a further temperature treatment above the regeneration temperature is stabilizing the reflectivity of an RFBG [13, 44, 52, 53]. This is in contradiction to a chemical-based RFBG theory, because here, the RFBG should decay continuously until it is erased. However, this observation is also difficult to explain on a crystallization-theory basis. These observations lend itself to the conclusion that RFBGs might be based on at least two physical effects, which affect the refractive index and have different temperature stabilities [42, 44].

In 2014 Yang et al. [54] reported that an RFBG with $\lambda_B = 1300$ nm already decays at 900 °C whereas an RFBG with $\lambda_B = 1550$ nm in the same fibre significantly loses reflectivity only at 1000 °C. This observation promotes both theories, because diffusion of O_2 or F_2, as well as crystal growth into the non-illuminated areas, will take longer when the grating pitch is higher.

3.3. The role of hydrogen and dopants during regeneration

The theories of Fokine and Canning where also challenged by investigations to identify and clarify the role of hydrogen during regeneration. It has been shown that it was not necessary that hydrogen was present during inscription. It has been demonstrated to be possible to regenerate FBGs in fibres that were hydrogenated *after* the inscription of the seed gratings [46, 52, 55]. Identically inscribed seed gratings without this "post hydrogen-loading" did not show any regeneration [55]. Canning interpreted this as an indication for mechanical relaxations due to the diffusion of hydrogen [47]. However, other measurements have shown, that an in- and out-diffusion of hydrogen before seed grating writing is not sufficient to allow regeneration at higher temperatures [22] (compare also Figure 3). This indicates that hydrogen molecules must interact with the UV inscription-induced changes in the glass. This can be argued to happen either physically by diffusion-induced mechanical relaxation of the glass structure as proposed by Canning [47] or chemically by hydrogen reactions with GODCs.

In 2009, Lindner et al. showed, that in fibres with very high Ge concentration, FBGs can regenerate even without hydrogen or helium loading [43]. This was confirmed in 2014 by Kumar et al. [56]. These observations are not covered by the differing theories proposed by Canning and Fokine. Fibres with highly Ge doped cores as used in Lindner's study are typically used for the inscription of type IIA gratings. Figure 6 shows an experiment, where the same highly Ge doped fibre was used as in [43] with 18% GeO_2-doping in the 5 µm diameter core (IPHT, Jena) and the same setups and H_2 loading conditions as in [22]. As can be seen, type IIA gratings in this fibre show regeneration without hydrogen, whereas type I gratings do not. This suggests that there is a fundamental connection between the ability of an FBG to regenerate and type IIA grating formation, at least in this special type of fibre. Although regenerated type IIA gratings and regenerated type I gratings with hydrogen show the same regeneration temperature of approximately 800 °C, they exhibit different thermal stabilities after regeneration. Therefore, it is reasonable to assume that there are different processes at work during regeneration of type I gratings in hydrogen loaded fibres and type IIA gratings in non-hydrogen loaded fibres.

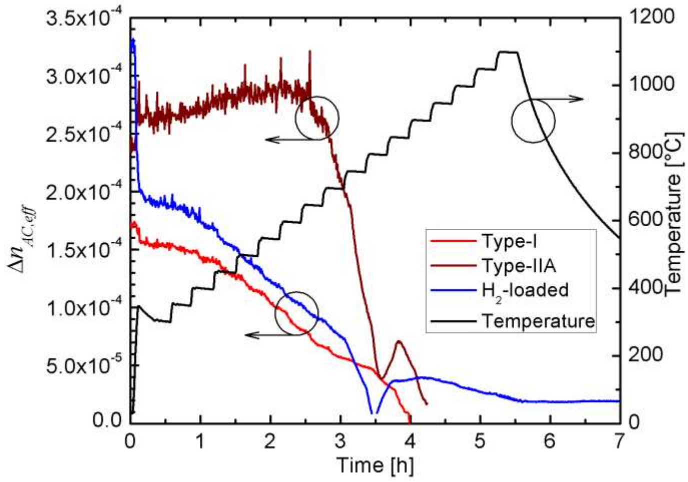

Figure 6: Comparison of the thermal behaviour of type I and type IIA gratings without H_2-loading and type I seed gratings in H_2-loaded fibre. The H_2-loaded and the type IIA FBGs regenerate at the same temperature, but show different thermal stabilities. The type I FBG without hydrogen shows no regeneration.

Other experiments focussed on the influence of different dopant compositions on regeneration. Although Ge-doping is helpful for seed grating inscription, it was shown not to be mandatory for regeneration of FBGs. Regeneration has been observed in fibres with Gallium doped [57] or mainly Zirconium doped [11] cores, and also in fibres consisting of a pure silica glass core and a fluorine doped depressed cladding [52]. It is noteworthy that the regeneration temperature is lower in fibres with higher dopant concentration [58-61]. Thus, it is apparent that the regeneration temperature is always in the same range as the expected glass transition temperature of the core material (compare also [11, 54]).

Experiments with hydrogen-loaded Ge-P-F co-doped fibre (GF1B, Nufern) have shown, that it is also possible to get an increase of grating reflectivity during thermal treatment even in two separated temperature regions (Figure 7) [32]. These temperature regions can be interpreted as two regeneration regimes. For the regeneration in both regimes prior hydrogen loading of the fibre is necessary. The GF1B fibre has a highly doped core and inner cladding, where the dopant composition and concentrations differ in both regions. Hence, the two regeneration regimes might be associated with two separate regeneration processes in the core and inner cladding that appear in two different temperature regions. This can be associated with either i) different glass transition temperatures of core and inner cladding, or ii) could be due to different stress distributions when compared to other fibres. Another characteristic of the GF1B fibre is the presence of fluorine inside its core and inner cladding. According to the observations of Fokine, an OH-driven diffusion of fluorine has to be expected between 500 °C and 700 °C (compare section 3.1), which can influence the refractive index modulation $\Delta n_{AC,eff}$. Therefore, it is also imaginable that the first regeneration might be based on F-diffusion as proposed by Fokine, and the second regeneration might be based on a crystallisation effect as proposed by Canning. Although the latter explanation is questioned by the observation of two regeneration regimes in B-Ge co-doped PS1250/1500 fibre (Fibrecore), which do not contain any fluorine, but a doped inner cladding [62, 63]. Chah et al. assume the reason for the first regeneration regime between 400 °C und 550 °C in PS1250/1500 is the boron annealing effect [63] which is based on the refractive index increase due to the release of frozen-in inelastic strain at the glass transition temperature [64, 65]. However, GF1B fibres do not contain any boron and the boron annealing effect also occurs without hydrogen loading [64]. Hence, further investigations have to be conducted to clarify the background and root causes of two regeneration regimes.

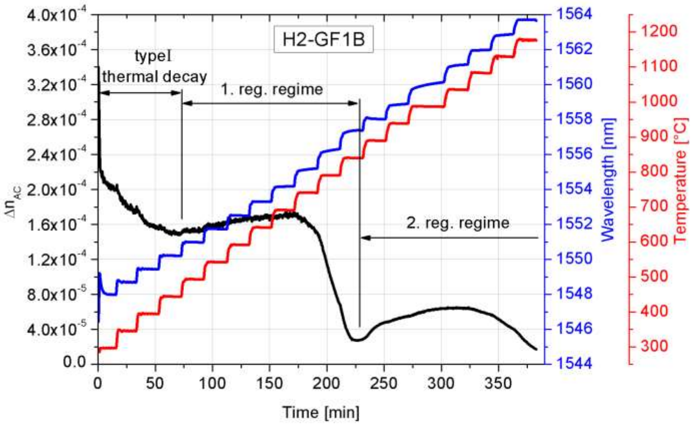

Figure 7: Regeneration of a Ge-P-F co-doped GF1B fibre (Nufern), showing two regeneration regimes, one between 500 °C to 700 °C and one between 850 °C to 1000 °C. (Graph adapted from [32])

3.4. Analysis of the refractive index change during regeneration

In 2014 Cheong et al. [66] and Holmberg et al. in 2015 [53] formulated similar hypotheses that the loss of reflectivity at the regeneration point might be caused by the refractive index change in the illuminated areas of the grating become negative ($\Delta n_{AC,eff} < 0$), similar to type II or type IIA gratings. As discussed in section 2.3, during type IIA grating inscription, at low cumulated fluence, a positive index change (type I part) is observed, before, at higher cumulated fluence, a negative index change (type II part) takes over. When the type II part of the grating reaches the same strength as the type I part, the grating shows nearly zero reflectivity (see Figure 4 and associated text). A similar process can be imagined to occur during the formation of an RFBG. During inscription of the seed grating, a type I FBG and a weak negative index part are produced simultaneously, but the type I part dominates strongly. When this grating is then heated, the type I FBG decays, while the negative index part stays constant (or at least decays much slower). At the regeneration point, type I and negative index part cancel each other out, because there is no longer a grating structure with the necessary periodicity and thus the grating reflectivity becomes zero. Afterwards, the reflectivity is regrowing, because the negative index part takes over. Such processes are already known from type IIA gratings. When type IIA gratings are heated, an increase in reflectivity is observed, because of the decaying type I FBG created at low fluence. If the type IIA grating inscription is stopped before the type II part becomes stronger than the type I part, and the grating is heated afterwards, even an evolution of the reflectivity with grating decay, vanishing reflectivity and regrow, can be achieved [67], similar to RFBGs.

One indication for the negative index hypothesis for RFBGs is the smooth trend of $\Delta n_{AC,eff}$ versus time during regeneration at constant temperature, using this assumption [53].

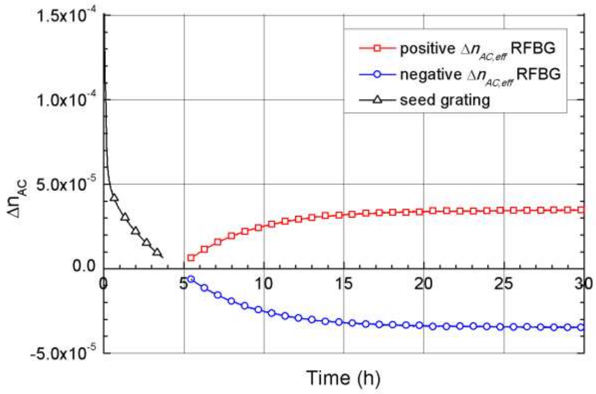

Figure 8: Evolution of $\Delta n_{AC,eff}$ during regeneration at constant temperature of 800 °C. The red squares curve shows the $\Delta n_{AC,eff}$ evolution with a positive continuation after regeneration, as assumed by the crystallization or the CCG theories. The blue circles curve instead shows the $\Delta n_{AC,eff}$ values taken after the grating has been regenerated but multiplied by a factor of -1, provided that $\Delta n_{AC,eff}$ is becoming negative during regeneration. Under this assumption, the graph shows a continuous transition through zero and exponential-like decay during the regeneration process.

Figure 8 shows the evolution of $\Delta n_{AC,eff}$ during regeneration with the grating held at a constant temperature, calculated from the measured reflectivity using Eq. (7). For the results shown in Figure 8 a H_2 loaded SMF28 fibre (Corning) was investigated using the same setup as described in [68]. Close to $\Delta n_{AC,eff} = 0$ data are missing because the reflected signal fell below the noise level. For the red (squares) values it was assumed that $\Delta n_{AC,eff}$ stays positive, whereas for the blue (circle) values $\Delta n_{AC,eff}$ was assumed to become negative for the RFBG. The blue (circles) curve shows a smooth continuation of the seed grating decay (black triangle), indicating there could be a negative $\Delta n_{AC,eff}$ offset from a more stable co-existing grating part. However, an argument against the negative index hypothesis is, that type IIA gratings, which are already negative index gratings, can still show regeneration (compare section 3.3).

When the positive type I part, introduced during inscription of the FBG, has totally vanished at higher temperatures and only the negative index part remains, the implication is that $\Delta n_{DC,eff}$ should become negative. This is a significant factor differentiating this hypothesis from the theories of Canning or Fokine, which both predict a positive $\Delta n_{AC,eff}$ and $\Delta n_{DC,eff}$ during RFBG growth. It was often tried to verify if $\Delta n_{DC,eff}$ is becoming negative during regeneration at constant temperature by observing the evolution of λ_B and using Eq. (2). However, positive [42-44, 48] as well as negative [60, 66, 69, 70] wavelength changes have been observed in these studies (also compare [53]). According to Eq. (2), not only $\Delta n_{DC,eff}$, but also n_{eff} and Λ_{FBG} have an influence on λ_B. Measurements in [31] show that the wavelength of an RFBG can be shifted by a few 100 pm by introducing and healing of frozen-in strain in the fibre since these affect n_{eff}. Since the regeneration of FBGs is mostly performed close to or above the glass transition temperature of the core, it is very likely that λ_B is not only affected by the change of $\Delta n_{DC,eff}$ due to the formation of the RFBG, but also due to changes in n_{eff} because of the healing of frozen-in stresses and strains (compare section 2). These frozen-in stresses and strains can increase or decrease n_{eff}, depending on the drawing conditions [29]. That these frozen-in stresses and strains are released during regeneration is also verified by the measurements of Kumar et al. [71]. Furthermore it was shown that the wavelength drift of high temperature FBGs does not depend on the type of FBG, but is more related to the used type of fibre [10, 72] and that there can be wavelength drifts without related changes in grating reflectivity [45]. All this indicates that the observed wavelength drifts are dominated by the annealing of frozen-in stresses and strains. In addition, a decrease in $\Delta n_{DC,eff}$ has to be taken into account during regeneration due to the decay of the seed grating and that λ_B will possibly change also by out-diffusion of remaining hydrogen. Hence it is very difficult to deduce the evolution of $\Delta n_{DC,eff}$ just from the observed changes in Bragg wavelength during regeneration.

3.5. Recent findings and outlook

Recently, it was found that the regeneration temperature is not a sharp threshold, but there is a wide temperature range over which a seed grating can regenerate [53, 73]. However, at lower temperatures the process of regeneration is much slower [74]. This effect can be explained with the O-CCG theory, because the diffusion constant of OH and H_2O increases with temperature [53]. Similarly, with a crystallization based theory this effect could be explained by the usually lower growth rate of seed crystals at lower temperatures [75]. It is not yet clear, if there is a low temperature limit for the regeneration, because at lower temperatures it can be necessary to wait 150 days until the grating regenerates [76].

Recent experiments using micro-Raman spectroscopy show that stress relaxation inside an RFBG is different to that in an annealed fibre without any FBG [77]. This opens avenues to new speculations that regeneration of FBGs could be based on the modulation of structural relaxation (density modulation) of the glass inside the fibre core. There are also other high temperature effects known from the literature, which are conceivably linked to the regeneration effect. For example, UV light can trigger a phase separation of GeO_2 und SiO_2 in Ge-doped silica [78] and also Zr-doped fibres show a phase separation as well as enhanced regeneration [79]. Unfortunately, a direct chemical or crystallographic measurement of the changes within the glass structure has not yet been published. As shown above, numerous investigations on the origin of the regeneration effect have been made, forming a broad base of knowledge about the regeneration effect in optical fibres. However, it must be accepted that the early CCG and crystallization theories both cannot comprehensively explain all the observed phenomena. In particular, the observation of RFBG formation in a fibre without cladding [51] is questioning the crystallization theory and the CCG theory cannot really explain the dependence of regeneration on the tension on the fibre [48, 49]. Moreover, the regeneration of gratings without hydrogen [43, 56] is in direct contradiction to both theories and raises the question of -*what is the role of hydrogen in the regeneration process?*. This does not indicate that the CCG theory and the crystallization theory are wrong, but rather that the final explanation of the regeneration effect might need a combination of multiple effects. This is underpinned by the observations presented in [32] and [13, 44, 52, 53], which also indicate that complex parallel processes are taking place during the formation of RFBGs.

4. Factors for tailored RFBG manufacturing

Even if the physical or chemical processes during RFBG formation are not yet fully understood, some distinct relations have been found which enable tailored RFBG manufacturing. It has been proven that, using well controlled parameters in manufacturing RFBGs, the final characteristics of reflectivity, wavelength and thermal stability can be reliably and repeatedly be reproduced [80]. Investigations have clearly identified key parameters, which strongly influence the regeneration temperature and strength of the RFBG. As already mentioned in section 3.3, it is possible to produce RFBG in many different types of fibres, but the amount of dopants is strongly affecting the regeneration process. Especially the regeneration temperature was found to be lower in fibres with higher dopant concentration [58-61] or, in other words, with core materials having lower transition temperatures. The required regeneration temperatures are ranging from 450 °C for highly B-Ge co-doped fibres [63], to 900 °C for standard SMF28 with approximately 3% GeO_2 [58] and up to 1200 °C for special Er-YZCAPS-fibres [11]. Thus, it is possible to choose the type of fibre according to the later maximum temperature in use.

An additional important finding is that with an equal temperature treatment for each grating, the strength of the RFBG is proportional to the strength of the seed grating [43, 58, 81]. Furthermore, this means that even the refractive index profile of the RFBG is a proportional replication of the seed grating. This characteristic allows the regeneration of complex grating structures such as superstructure or chirped FBGs [44, 82]. In the same way it was possible to produce tilted RFBG [83] and regenerated long period gratings [84, 85]. Hence, the maximum reachable $\Delta n_{AC,eff}$ of an RFBG only seems to be limited by the highest possible strength of the seed grating. This is demonstrated by the ability to produce RFBG with $\Delta n_{AC,eff} > 1\cdot 10^{-4}$ [22, 53, 86].

Lindner has defined the regeneration efficiency as

$$regen\ eff' = \Delta n_{AC,eff,RFBG} / \Delta n_{AC,eff,seed}, \qquad (13)$$

and has observed efficiencies in the order of 10% to 14% for his gratings [87]. However, calculating the regeneration efficiency for other measurements in the literature, it can be seen that the values are strongly deviating from the ratio measured by Lindner, ranging up to ratios of 72% for the regeneration efficiency observed in a special Er-ZYAG fibre [79]. In some publications it was supposed that the strength of the RFBG is related to the content of Ge within the fibre core [58, 59]. Figure 9 shows a comparison of the regeneration behaviour of two types of fibres with strongly differing Ge concentration during slow isochronal heating. For the experiment seed gratings with similar strength were inscribed in H_2-loaded SMF28 fibre (approx. 3% GeO_2) and H_2-loaded PR fibre (approx. 18% GeO_2). The test was performed in a metal block calibration furnace (Pegasus Plus 1200 S, Isotech Ltd.) with a heating rate of two Kelvin per minute (A detailed description of the test can be found in [88]). It can be seen, that the regeneration efficiency is not depending on the amount of Ge within the fibre, but just the regeneration temperature is different [88].

To achieve maximum regeneration ratios, it is important that there is no remaining hydrogen within the fibre during regeneration. For example, if the fibre is heated very quickly, remaining hydrogen can thermally produce OH groups, additionally to the UV-induced ones, which are then spread homogeneously within the whole fibre, decreasing the contrast between the illuminated and non-illuminated areas of the FBG [7, 25], obstructing regeneration [12, 25]. This might also be the reason, why in early publications it was reported that a fast heating of the seed grating hampers regeneration [40, 89]. That this is in fact not the case was shown by Bueno et al. [60]. They have heated seed gratings by fast immersion into a preheated furnace and the gratings regenerated. However these fast immersion regenerated gratings are slightly weaker compared to regenerated gratings using a low temperature ramp rate. Different pre-annealing at lower temperatures before regeneration, however, was observed to influence the regeneration only marginal [90].

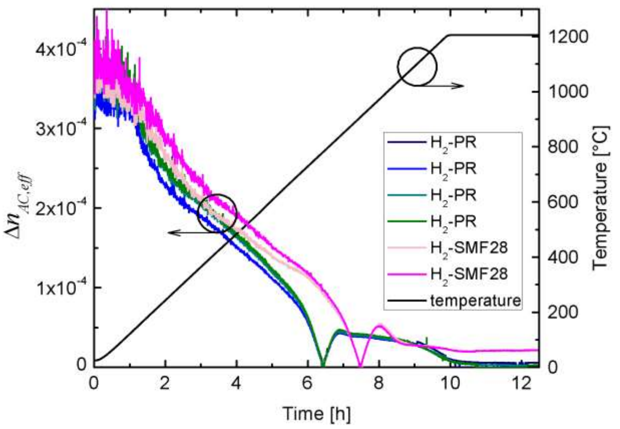

Figure 9: Comparison of the regeneration behaviour of seed gratings in hydrogen-loaded fibres with different Ge-concentration within the core during slow isochronal heating. The gratings in the different fibres regenerate at different temperatures but the maximal reached strength of all RFBGs is the same.

Higher hydrogen concentrations inside the fibre, determined by the hydrogen pressure and temperature during H_2-loading (compare section 2), have been reported to result in an increased regeneration efficiency [81]. For most of the published regeneration experiments in hydrogen-loaded fibres, H_2 loading pressures between 100 bar and 200 bar at temperatures up to 100 °C were used. But there have also been RFBGs in fibres, which were only loaded with 25 bar of hydrogen pressure at room temperature for two weeks [91]. However, a detailed study regarding the correlation between regeneration efficiency and hydrogen pressure is not known.

A comparison of the regeneration efficiency for different wavelengths used for seed grating inscription is also not known. However, there is no reference for any dependency on inscription wavelength, because there have been successful regenerations of seed gratings written with many different laser sources, e.g. with fs-lasers with 800 nm [52] or 266 nm [92] wavelength, or with ns pulses at UV wavelengths of 255 nm [56], 248 nm [10, 22, 31, 32, 43, 48, 55, 59, 69, 82, 86-88, 93-102], 244 nm [11, 12, 37, 40, 44, 45, 51, 54, 60, 61, 66, 72, 83, 91, 103-105], 240 nm [33], 213 nm [53], and 193 nm [41, 46, 49, 57, 73, 76, 80, 81, 85, 89, 106-113]. Furthermore, the energy density, which is used to inscribe the seed grating, is also not affecting the regeneration efficiency [81]. Table 2 summarizes the known main parameters and their effect on regeneration of FBGs.

Table 2. Regeneration parameters and their effect on RFBGs

Parameter	Effect
Higher Ge-concentration	Lower regeneration temperature or faster regeneration. Lower thermal stability. [11, 58-61]
Type of dopants	Influence on regeneration efficiency and regeneration temperature, probably related with glass transition temperature. [58, 61, 79]
Higher Seed grating strength	Higher RFBG grating strength. [43, 58, 81].
Longer Grating wavelength	Slower RFBG decay. [54]

5. Applications and application-related investigations

Over the past 20 years, the suitability of RFBGs as temperature sensors for high temperature applications have been investigated where RFBGs have been used to, for example, measure the temperature during diamond deposition in a vacuum chamber [114], or during the manufacturing of fibre preforms on the inner side of the preform [106]. The suitability to monitor temperatures with RFBGs in the case of building fires was shown by Rinaudo [115]. In order to measure with RFBGs at different positions at the same time, common wavelength multiplexing methods can be used [93]. Figure 10, for example, shows an array of 6 gratings with different λ_B along one single fibre before and after regeneration (graph taken from [68]). As can be seen, after regeneration every single Bragg reflection peak, although reduced in intensity, is still clearly detectable with good signal to noise ratio. With such RFBG arrays, e.g. the temperature distribution in a furnace [103], in a soot blower [13], in a chemical reaction vessel [68], in the exhaust duct of gas turbines [10, 116, 117], in liquid Sodium [72], or within solidifying aluminium [118, 119] was measured. To our knowledge, no enhanced cladding or radiation mode losses have ever been observed for RFBGs when compared with its type I seed FBGs (see also [83] or [85]). Therefore, the same multiplexing capabilities apply to RFBGs as for type I FBGs.

The fact that the wavelength response to temperature of each RFBG in the same type of fibre is equal, is very helpful for the usage of RFBG arrays, because it means that not every RFBG has to be calibrated separately, but just a single temperature calibration point, e.g. at room temperature, is sufficient [119]. Direct comparison of RFBG-based temperature measurements within gas turbines with commonly used thermocouples showed that, using RFBG arrays, a higher spatial density of measurement points with equal accuracy was feasible. Due to the faster response time of RFBGs, dynamic temperature and vibration analysis was possible [117]. However, the ability to use RFBGs close to radioactive sources and X-rays appear to be limited since they exhibit higher wavelength drifts, especially at low temperatures, in these environments [72, 120].

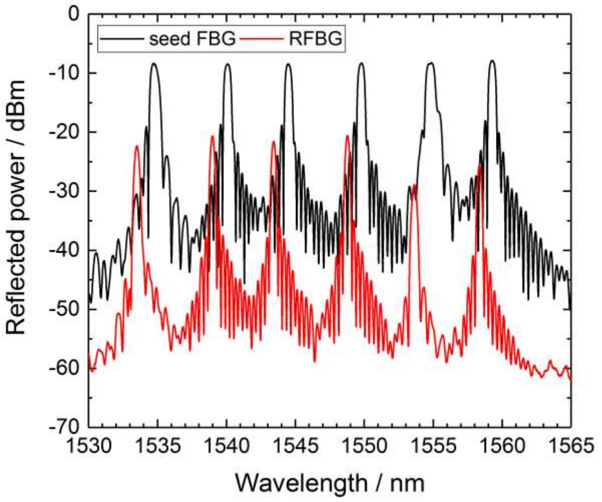

Figure 10: Spectra of a multiplexed RFBG array, within a single fibre, before and after regeneration. (Graph taken from [68])

RFBG are also suitable for long time measurements. For example, four RFBG arrays have been applied in a chemical test reactor for two years measuring temperatures in the range of 150 °C to 500 °C, and without showing any failure or significant wavelength drift [68]. Laffont et al. have annealed RFBGs in a high temperature furnace at 760 °C to 900 °C for one year [45]. However, in this study, the RFBGs have shown a drift in wavelength, but just minor changes in reflectivity. It was also apparent, that the drift of the RFBGs diminishes over time, which indicates that pre-annealing processes can be applied to RFBGs, similar to those used for precise high temperature thermocouples. This fits to the assumption that the wavelength drift originates from frozen-in stresses and strains, which have to be healed out to reach more stable conditions (compare section 3.4). The long term drift of intense pre-annealed RFBGs was investigated by Xia [13]. He annealed an RFBG at 1100 °C for 12 hours. Thereafter, the drift was reduced to $1.2\cdot10^{-3}$ nm/h at 1000 °C within 300 min, which corresponds to an increasing temperature uncertainty of approximately 70 mK/h. In addition, it has to be taken into account that above the glass transition temperature fast temperature changes will lead to thermally induced strain in the glass structure of the fibre core [31]. At high temperatures this strain is then released over time, which can cause wavelength drift. This means that measurements with fast temperature changes above the transition temperature of the core glass could be biased. In the region of the glass transition temperature, the mechanical behaviour of the glass is changing from pure elastic to viscoelastic, which means that force or strain measurements with RFBG will also be affected by drifts [121]. If the temperature is reaching the transition temperature of the cladding, the complete fibre is softening and can be elongated by even a small tensile force, which changes the grating period and thereby induces a wavelength drift [49]. On the other hand, this effect can be used to adjust the wavelength of the RFBGs after regeneration. This property was used to measure the viscosity of fibre glass at temperatures between 1000 °C and 1150 °C [110], or to produce chirped RFBGs by applying a temperature gradient to the RFBG together with a constant tension on the fibre [107].

Environments with a high pH above 7 [122], humidity [123], and high temperature surface crystallization [124] can lead to strong corrosion of optical fibres. To protect RFBG sensors from such environmental effects, they are usually inserted into steel capillaries [10, 68, 72, 91, 109, 117-119]. Especially for long sensor arrays, this can lead to friction-induced measurement errors [118, 125]. The effect of high temperature corrosion during regeneration on the mechanical stability of the fibre was investigated by Wang et al. [112]. They measured the change of breaking elongation of the fibre due to the regeneration process, which lasted 40 min at 850 °C. It was observed, that the temperature treatment reduces the maximum applicable strain to approx. a third of the value of an untreated fibre. However, the mechanical stability of RFBGs is still sufficient to use them as strain or force sensors [62, 100, 105, 113, 126, 127]. For example, RFBGs have been re-coated with Polyimide and glued with epoxy onto a metal plate to create a strain sensor which is suitable for up to 400 °C [105]. By using high temperature adhesives, it was even possible to realize strain measurements with RFBGs at up to 1000 °C [126]. Due to the temperature stability of the RFBG it is also possible to implement the RFBG directly into metallic components during casting [127]. For fibre optic strain sensors, which should be embedded into metallic structures, it is helpful to have a metallic coating to improve the adhesion between fibre and metallic bulk. But also in general, a metallic coating can help to improve the mechanic stability of the fibre and the temperature sensitivity of the RFBG. For example RFBGs have been sputtered with a smooth layer of 500 nm silver [111]. Such a thin metallic coating is not changing the temperature response of the RFBG and can be used as protective coating up to 600 °C. Care has to be taken that the metallic coating itself is not too thick as to induce thermally induced strain in the fibre due to the large mismatch in CTE between a fused silica fibre and any metallic coating. Further experiments have been made with a three layer coating composed of 100 nm titanium, 500 nm silver and 200 µm nickel and have also shown a good bonding of the coating up to 600 °C and a duplication of the temperature sensitivity of the RFBG [128]. With such a coated RFBG a weldable strain sensor was developed and tested up to 540 °C and up to 800 micro strain [62].

Especially for embedded RFBGs, but also for long arrays in capillaries, there is the problem to differentiate between wavelength shifts induced by temperature or by strain. To solve this problem, it is possible to separate both effects by combining two closely spaced sensors, exposed to the same temperature, which comprise different sensitivities to both parameters. This concept has been widely demonstrated using conventional FBGs and has also been demonstrated by using a combination of two RFBGs with different λ_B [101] or different fibre diameters [129] and using a combination of an RFBG together with a Fabry-Pérot cavity [98, 108]. Another possibility is to use RFBGs in polarisation maintaining (PM) fibres with stress induced birefringence [100]. These fibres contain stress applying regions, commonly made of highly boron doped glass. This limits their usable temperature range below the glass transition temperature of the boron doped regions, which is typically around 500 °C. Fibres with structural induced birefringence, in contrast, normally do not contain highly boron doped glass and are therefore usable up to higher temperatures [130]. However, these fibres show also just a weak change of birefringence with temperature or strain, and therefore they are not an appropriate solution for simultaneous temperature and strain measurements. In contrast, using an RFBG in a special twin-air-hole PM fibre with structural induce birefringence, it was possible to realize a sensor for simultaneous temperature and pressure sensing up to 800 °C, because this fibre shows a great sensitivity of the birefringence to external pressure changes [69].

Beside the usage as temperature or strain sensors, RFBG can also be envisaged in every other FBG-based device to improve its high temperature capability. For example, a high temperature stable fibre laser using two RFBGs was developed and successfully tested at 750 °C [94] and by combination of two RFBGs in different types of fibres, it was possible to realize a high temperature stable flow sensor based on the principle of a hot wire anemometer [95].

6. Conclusion

Over more than two decades, many investigations on regenerated FBGs in different types of fibres and with different pre-treatments before regeneration have been performed, creating a broad base of knowledge, which is of great benefit for the tailored manufacturing and application of RFBG. Shortly after the first studies, two alternative theories, the crystallisation theory and the chemical composition theory, have been established, with both being supported by different experimental observations and neither of them having been disproved to date. However, both theories struggle to explain the regeneration phenomena in its whole complexity and in particular fail to explain observation of RFBG in fibres without hydrogen loading [43, 56]. Recent measurements using micro-Raman spectroscopy [77] and the indication that the regeneration temperature seems to follow the glass transition temperature of the fibre core, give hints towards a relation between regeneration and stress relaxation effects. However, especially observations like the regeneration in two different temperature regimes [32, 62, 63] or the often observed graduated decay of RFBG [13, 44, 52, 53] indicates that multiple processes might be active in parallel, which might show different temperature dependencies.

Many experiments have identified specific parameters, which critically influence the regeneration behaviour of FBGs. Most importantly, the strength of the seed grating determines the final strength of the RFBG and the dopant material (mostly Ge) and concentration determines the temperature region in which the gratings can regenerate within a reasonable period.

The reflectivity of RFBGs has been shown to be quite stable, especially when the temperature stays below the regeneration temperature. Above the regeneration temperature and above the glass transition temperature of the core material, an RFBG can still survive for some hours, but a continuous change in grating properties has to be expected, limiting the usability of the RFBG e.g. as temperature or strain sensors. On the other hand, this can be used to measure the glass properties or tailor the reflection spectrum of the RFBG.

Besides the intensively investigated and confirmed stability in reflectivity, an essential aspect for using RFBGs as sensors must be considered, namely the wavelength stability of the RFBGs. It has been shown, that below the regeneration temperature, despite showing stable reflectivity, RFBGs are showing a very small but measurable drift in wavelength similar to other high temperature FBGs, which might be appreciable in long term measurements. Some investigations indicate that the drift can be reduced by annealing processes similar to those used for thermocouples. However, the reasons for the observed drift and its dependencies on temperature or fibre composition are not yet fully understood and the rates of drift vary depending on fibre type, regeneration temperature and thermal history. It is essential that future investigations on RFBG should address this topic to enable and strengthen the use of RFBGs for high temperature sensing applications.

Nevertheless, despite the uncertainties in the processes leading towards the creation of RFBG, those, skilled in the art, are able to reliably, reproducibly and efficiently create high temperature stable RFBGs, which can and already have been employed successfully in industrial applications, showing that the technique is suitable for commercial use.

There are numerous engineering applications which are in urgent need of high temperature capable strain sensing elements. For example, stress corrosion cracking is a critical failure mechanism in high temperature steam systems, currently limiting the upper operation temperatures of steam driven power generation systems, thus limiting improvements in energy efficiency. There are currently no reliable long-term sensor systems available for this application and RFBGs are getting close to the required specification in stability but are not there yet.

A future detailed understanding of the underlying theory or theories, depending on fibre type and processes employed, of course, will help and further the uptake of this important sensor technology by assisting in optimising the stability and reliability of these sensor components.

Acknowledgements

This work was supported by the German Minister of Research and Technology under FKZ 170 10X 11 and the Bavarian Research Foundation under grant number AZ-1146-14.

References

[1] I. Bennion, J.A.R. Williams, L. Zhang, K. Sugden, N.J. Doran, UV-written in-fibre Bragg gratings, Opt. Quant. El. 28(2) (1996) pp. 93-135, https://doi.org/10.1007/BF00278281.

[2] J. Canning, New Fibre and Grating Technologies for Lasers and Sensors, in: W.T. Arkin (Ed.) Frontiers in Laser and Electro-Optics Research, Nova Science Publishers, New York, 2006, p. 62, ISBN 1-59454-770-X.

[3] B. Lee, Review of the present status of optical fiber sensors, Opt. Fiber Tech. 9 (2003) pp. 57-79, https://doi.org/doi:10.1016/S1068.

[4] K.O. Hill, Y. Fujii, D.C. Johnson, B.S. Kawasaki, Photosensitivity in optical fiber waveguides: Application to reflection filter fabrication, Appl. Phys. Lett. 32(10) (1978) pp. 647-649, https://doi.org/10.1063/1.89881.

[5] G. Meltz, W.W. Morey, W.H. Glenn, Formation of Bragg gratings in optical fibers by a transverse holographic method, Optics letters 14(15) (1989) pp. 823-825, https://doi.org/10.1364/OL.14.000823.

[6] K.O. Hill, B. Malo, F. Bilodeau, D.C. Johnson, J. Albert, Bragg gratings fabricated in monomode photosensitive optical fiber by UV exposure through a phase mask, Appl. Phys. Lett. 62(10) (1993) pp. 1035-1037, https://doi.org/10.1063/1.108786.

[7] J. Canning, Fibre gratings and devices for sensors and lasers, Laser and Photonics Review 2(4) (2008) pp. 275-289, https://doi.org/10.1002/lpor.200810010.

[8] J. Canning, M. Stevenson, K. Cook, M. Aslund, W. Ecke, R. Willsch, H. Bartelt, H.J. Kalinowski, L. Grabarski, V. Oliveira, C. Martelli, A. Braga, N. Groothoff, G.-D. Peng, Optical fibre Bragg gratings for high temperature sensing, in: J.D.C. Jones, B. Culshaw, W. Ecke, J.M. Lopez-Higuera, R. Willsch (Eds.) 20th International Conference on Optical Fibre Sensors, SPIE, 2009, pp. 75032N-4, https://doi.org/10.1117/12.834470.

[9] T. Erdogan, V. Mizrahi, P.J. Lemaire, D. Monroe, Decay of ultraviolet-induced fiber Bragg gratings, J. App. Phys 76(1) (1994) pp. 73-80, https://doi.org/10.1063/1.357062.

[10] F.J. Dutz, M. Lindner, A. Heinrich, C.G. Seydel, T. Bosselmann, A.W. Koch, J. Roths, Multipoint high temperature sensing with regenerated fiber Bragg gratings, Fiber Optic Sensors and Applications XV, International Society for Optics and Photonics, 2018, p. 1065407, https://doi.org/10.1117/12.2305300.
[11] H.Z. Yang, X.G. Qiao, S. Das, M.C. Paul, Thermal regenerated grating operation at temperatures up to 1400 degrees C using new class of multimaterial glass-based photosensitive fiber, Optics letters 39(22) (2014) pp. 6438-6441, https://doi.org/10.1364/OL.39.006438.
[12] M. Fokine, Growth dynamics of chemical composition gratings in fluorine-doped silica optical fibers, Optics letters 27(22) (2002) pp. 1974-1976, https://doi.org/10.1364/OL.27.001974.
[13] H. Xia, Advanced Fiber Optical Sensor and Instrumentation for Power Generation Industrial Monitoring and Diagnostics, in: H.H. Du, G. Pickrell, E. Udd, J.J. Benterou, A. Mendez, S.J. Mihailov, A. Wang (Eds.) Fiber Optic Sensors and Applications IX, SPIE, 2012, pp. 83700F-10, https://doi.org/10.1117/12.922587.
[14] H. Xia, K.T. McCarthy, K.-L.J. Deng, F.J. Lopez, A.J. Avagliano, Fiber Bragg Grating for high temperature sensing, United States Patent, US 7,499,605 B1, General Electric Company, Niskayuna, NY, USA, 2009.
[15] S.J. Mihailov, Fiber Bragg Grating Sensors for Harsh Environments, Sensors 12(2) (2012) pp. 1898-1918, https://doi.org/10.3390/s120201898.
[16] A. Martinez, M. Dubov, I. Khrushchev, I. Bennion, Direct writing of fibre Bragg gratings by femtosecond laser, Elec. Lett. 40(19) (2004) p. 1170, https://doi.org/10.1049/el:20046050.
[17] R. Kashyap, Fiber Bragg gratings, 2. Ed. ed., Academic, London, 2010, ISBN 978-0-12-372579-0.
[18] A. Othonos, K. Kalli, Fiber Bragg gratings: Fundamentals and applications in telecommunications and sensing, Artech House, Boston, MA, 1999, ISBN 0-89006-344-3.
[19] T. Erdogan, Fiber grating spectra, Journal of Lightwave Technology 15(8) (1997) pp. 1277-1294, https://doi.org/10.1109/50.618322.
[20] M. Lancry, B. Poumellec, UV laser processing and multiphoton absorption processes in optical telecommunication fiber materials, Phys. Rep. 523(4) (2013) pp. 207-229, https://doi.org/10.1016/j.physrep.2012.09.008.
[21] J. Rathje, M. Kristensen, J.E. Pedersen, Continuous anneal method for characterizing the thermal stability of ultraviolet Bragg gratings, J. App. Phys 88(2) (2000) pp. 1050-1055, https://doi.org/10.1063/1.373775.
[22] L. Polz, A. Dörfler, H. Bartelt, J. Roths, Regeneration experiments with fibre Bragg gratings in hydrogen outdiffused fibres, in: J.M. López-Higuera, J.D.C. Jones, M. López-Amo, J.L. Santos (Eds.) 23rd International Conference on Optical Fibre Sensors, SPIE, Santander, 2014, pp. 91577F-4, https://doi.org/10.1117/12.2059552.
[23] P.L. Swart, A.A. Chtcherbakov, Study of hydrogen diffusion in boron/germanium codoped optical fiber, Journal of Lightwave Technology 20(11) (2002) pp. 1933-1941, https://doi.org/10.1109/JLT.2002.806325.
[24] P.L. Swart, A.A. Chtcherbakov, W.L. Joubert, M.G. Shlyagin, Study of the pressure dependence of hydrogen diffusion in optical fiber by an interferometric technique, Optics Communications 217(1-6) (2003) pp. 189-196, https://doi.org/10.1016/S0030-4018(03)01107-6.
[25] M. Fokine, Photosensitivity, chemical composition gratings and optical fiber based components, PhD Thesis, Royal Institute of Technologie, Stockholm, 2002, ISBN 91-7283-397-1.
[26] M. Fokine, H. Suzuki, T. Goto, K. Saito, A.J. Ikushima, High-temperature treatment of hydrogen loaded GeO_2:SiO_2 glasses for photonic device fabrication, Journal of Non-Crystalline Solids 352(6-7) (2006) pp. 494-499, https://doi.org/10.1016/j.jnoncrysol.2005.11.037.
[27] N.H. Ky, H.G. Limberger, R.P. Salathé, F. Cochet, L. Dong, UV-irradiation induced stress and index changes during the growth of type-I and type-IIA fiber gratings, Optics Communications 225(4-6) (2003) pp. 313-318, https://doi.org/10.1016/j.optcom.2003.07.039.
[28] S.A. Kukushkin, M.G. Shlyagin, P.L. Swart, A.A. Chtcherbakov, A.V. Osipov, Type IIA photosensitivity and formation of pores in optical fibers under intense ultraviolet irradiation, J. App. Phys 102(5) (2007) pp. 053502-13, https://doi.org/10.1063/1.2773996.
[29] A.D. Yablon, Optical and Mechanical Effects of Frozen-in Stresses and Strains in Optical Fibers, IEEE J. Sel. Topics Quantum Electron. 10(2) (2004) pp. 300-311, https://doi.org/10.1109/jstqe.2004.826570.
[30] F. Just, R. Spittel, J. Bierlich, S. Grimm, M. Jäger, H. Bartelt, The influence of the fiber drawing process on intrinsic stress and the resulting birefringence optimization of PM fibers, Optical Materials 42 (2015) pp. 345-350, https://doi.org/10.1016/j.optmat.2015.01.025.
[31] M.-H. Lai, K.-S. Lim, D.S. Gunawardena, H.-Z. Yang, W.-Y. Chong, H. Ahmad, Thermal stress modification in regenerated fiber Bragg grating via manipulation of glass transition temperature based on CO_2 laser annealing, Optics letters 40(5) (2015) pp. 748-751, https://doi.org/10.1364/OL.40.000748.
[32] L. Polz, Q. Nguyen, H. Bartelt, J. Roths, Fiber Bragg gratings in hydrogen-loaded photosensitive fiber with two regeneration regimes, Optics Communications 313 (2014) pp. 128-133, https://doi.org/10.1016/j.optcom.2013.09.061.
[33] M. Fokine, B.E. Sahlgren, R. Stubbe, A Novel Approach to Fabricate High-Temperature Resistant Fiber Bragg Gratings, Bragg Gratings, Photosensitivity, and Poling in Glass Waveguides (BGPP), Optical Society of America, Washington, DC, 1997, pp. 58-60, ISBN 1-55752-517-X.
[34] M. Hellsing, M. Fokine, Å. Claesson, L.-E. Nilsson, W. Margulis, ToF-SIMS imaging of dopant diffusion in optical fibers, App. Surf. Sci. 203-204 (2003) pp. 648-651, https://doi.org/10.1016/S0169-4332(02)00783-3.
[35] M. Fokine, Formation of thermally stable chemical composition gratings in optical fibers, J. Opt. Soc. Am. B 19(8) (2002) pp. 1759-1765, https://doi.org/10.1364/JOSAB.19.001759.
[36] M. Fokine, Underlying mechanisms, applications, and limitations of chemical composition gratings in silica based fibers, Journal of Non-Crystalline Solids 349 (2004) pp. 98-104, https://doi.org/10.1016/j.jnoncrysol.2004.08.208.
[37] M. Fokine, Thermal stability of chemical composition gratings in fluorine-germanium-doped silica fibers, Optics letters 27(12) (2002) pp. 1016-1018, https://doi.org/10.1364/OL.27.001016.
[38] M. Fokine, Thermal stability of oxygen-modulated chemical-composition gratings in standard telecommunication fiber, Optics letters 29(11) (2004) pp. 1185-1187, https://doi.org/10.1364/OL.29.001185.
[39] M. Fokine, I. Miyamoto, A. Ostendorf, K. Sugioka, H. Helvajian, Laser Induced Sub-micron Changes of the Chemical Composition of Si02-based Optical Fibers, in: I. Miyamoto, A. Ostendorf, K. Sugioka, H. Helvajian (Eds.) Fourth International Symposium on Laser Precision, SPIE, 2003, pp. 453-462, https://doi.org/10.1117/12.541170.
[40] S. Trpkovski, D.J. Kitcher, G.W. Baxter, S.F. Collins, S.A. Wade, High-temperature-resistant chemical composition Bragg gratings in Er3+-doped optical fiber, Optics letters 30(6) (2005) pp. 607-609, https://doi.org/10.1364/OL.30.000607.
[41] J. Canning, M. Stevenson, S. Bandyopadhyay, K. Cook, Extreme Silica Optical Fibre Gratings, Sensors 8(10) (2008) pp. 6448-6452, https://doi.org/10.3390/s8106448.
[42] J. Canning, S. Bandyopadhyay, P. Biswas, M. Aslund, M. Stevenson, K. Cook, Regenerated Fibre Bragg Gratings, in: B. Pal (Ed.) Frontiers in Guided Wave Optics and Optoelectronics, INTECH, Croatia, 2010, p. 22, ISBN 978-953-7619-82-4.
[43] E. Lindner, C. Chojetzki, S. Brückner, M. Becker, M. Rothhardt, H. Bartelt, Thermal regeneration of fiber Bragg gratings in photosensitive fibers, Opt. Exp. 17(15) (2009) pp. 12523-12531, https://doi.org/10.1364/OE.17.012523.
[44] J. Canning, S. Bandyopadhyay, M. Stevenson, P. Biswas, J. Fenton, M. Aslund, Regenerated gratings, J. Europ. Opt. Soc. - Rap. Pub. 4 (2009) pp. 09052-7, https://doi.org/10.2971/jeos.2009.09052.
[45] G. Laffont, R. Cotillard, P. Ferdinand, 9000 hours-long high temperature annealing of regenerated fiber Bragg gratings, in: L.R. Jaroszewicz (Ed.) Fifth European Workshop on Optical Fibre

Sensors, SPIE, Krakow, 2013, pp. 87941X-4, https://doi.org/10.1117/12.2025838.
[46] K. Cook, L.-Y. Shao, J. Canning, Regeneration and helium: regenerating Bragg gratings in helium-loaded germanosilicate optical fibre, Optical Materials Express 2(12) (2012) pp. 1733-1742, https://doi.org/10.1364/OME.2.001733.
[47] J. Canning, Regeneration, regenerated gratings and composite glass properties: the implications for high temperature micro and nano milling and optical sensing, Measurement (2015), https://doi.org/http://dx.doi.org/10.1016/j.measurement.2015.09.020.
[48] E. Lindner, J. Canning, C. Chojetzki, S. Brückner, M. Becker, M. Rothhardt, H. Bartelt, Thermal regenerated type IIa fiber Bragg gratings for ultra-high temperature operation, Optics Communications 284(1) (2011) pp. 183-185, https://doi.org/10.1016/j.optcom.2010.08.075.
[49] T. Wang, L.-Y. Shao, J. Canning, K. Cook, Regeneration of fiber Bragg gratings under strain, Applied optics 52(10) (2013) pp. 2080-2085, https://doi.org/10.1364/AO.52.002080.
[50] G. Violakis, N. Aggarwal, H.G. Limberger, Stress changes in H2-loaded SMF optical fibers induced by cw-Ar 244 nm irradiation, Optical Materials Express 2(11) (2012) pp. 1490-1495, https://doi.org/10.1364/OME.2.001490.
[51] H. Yang, W.Y. Chong, Y.K. Cheong, K.-S. Lim, C.H. Pua, S.W. Harun, H. Ahmad, Thermal Regeneration in Etched-Core Fiber Bragg Grating, IEEE Sensors J. 13(7) (2013) pp. 2581-2585, https://doi.org/10.1109/jsen.2013.2256344.
[52] K. Cook, C. Smelser, J. Canning, G. Le Garff, M. Lancry, S. Mihailov, Regenerated femtosecond fibre Bragg gatings, in: J. Canning, G. Peng (Eds.) 3rd Asia Pacific Optical Sensors Conference, SPIE, 2012, pp. 835111-6, https://doi.org/10.1117/12.915937.
[53] P. Holmberg, F. Laurell, M. Fokine, Influence of pre-annealing on the thermal regeneration of fiber Bragg gratings in standard optical fibers, Opt. Exp. 23(21) (2015) pp. 27520-27535, https://doi.org/10.1364/OE.23.027520.
[54] H.-Z. Yang, W.-Y. Chong, X.-G. Qiao, M.-J. Lim, K.-S. Lim, M.R. Islam, N.M. Ali, H. Ahmad, 1.3 and 1.55 µm Thermally Regenerated Gratings in Hydrogenated Boron/Germanium Co-Doped Photosensitivity Fiber, IEEE Sensors J. 14(5) (2014) pp. 1352-1356, https://doi.org/10.1109/jsen.2013.2294973.
[55] E. Lindner, J. Canning, C. Chojetzki, S. Brückner, M. Becker, M. Rothhardt, H. Bartelt, Post-hydrogen-loaded draw tower fiber Bragg gratings and their thermal regeneration, Applied optics 50(17) (2011) pp. 2519-2522, https://doi.org/10.1364/AO.50.002519.
[56] J. Kumar, R. Mahakud, A. Mokhariwale, O. Prakash, S.K. Dixit, S.V. Nakhe, Studies on thermal regeneration and temperature stability of type-I FBGs written in Ge-B codoped and Ge doped fibers by a kHz repetition rate nanosecond 255nm beam, Optics Communications 320 (2014) pp. 109-113, https://doi.org/10.1016/j.optcom.2014.01.049.
[57] D.S. Gunawardena, K.A. Mat-Sharif, M.-H. Lai, K.-S. Lim, N. Tamchek, N.Y.M. Omar, S.D. Emami, S.Z. Muhamad-Yasin, M.I. Zulkifli, Z. Yusoff, H.-Z. Yang, H.A. Abdul-Rashid, H. Ahmad, Thermal Activation of Regenerated Grating in Hydrogenated Gallosilicate Fiber, IEEE Sensors J. 16(6) (2016) pp. 1659-1664, https://doi.org/10.1109/jsen.2015.2503438.
[58] S. Bandyopadhyay, J. Canning, P. Biswas, M. Stevenson, K. Dasgupta, A study of regenerated gratings produced in germanosilicate fibers by high temperature annealing, Opt. Exp. 19(2) (2011) pp. 1198-1206, https://doi.org/10.1364/OE.19.001198.
[59] J.-J. Zhu, A.P. Zhang, B. Zhou, F. Tu, J.-T. Guo, W.-J. Tong, S. He, W. Xue, Effects of doping concentrations on the regeneration of Bragg gratings in hydrogen loaded optical fibers, Optics communications 284(12) (2011) pp. 2808-2811, https://doi.org/10.1016/j.optcom.2011.01.074.
[60] A. Bueno, D. Kinet, P. Megret, C. Caucheteur, Fast thermal regeneration of fiber Bragg gratings, Optics letters 38(20) (2013) pp. 4178-4181, https://doi.org/10.1364/OL.38.004178.
[61] D. Barrera, Fiber-optic sensors for high-temperature applications, SPIE Newsroom (2010) p. 2, https://doi.org/10.1117/2.1201003.002676.
[62] Y. Tu, L. Ye, S.-P. Zhou, S.-T. Tu, An Improved Metal-Packaged Strain Sensor Based on A Regenerated Fiber Bragg Grating in Hydrogen-Loaded Boron–Germanium Co-Doped Photosensitive Fiber for High-Temperature Applications, Sensors 17(3) (2017) p. 431, https://doi.org/10.3390/s17030431.
[63] K. Chah, K. Yuksel, D. Kinet, N.S. Yazd, P. Megret, C. Caucheteur, Fiber Bragg grating regeneration at 450 degrees C for improved high temperature sensing, Optics letters 44(16) (2019) pp. 4036-4039, https://doi.org/10.1364/OL.44.004036.
[64] I. Camlibel, D.A. Pinnow, F.W. Dabby, Optical aging characteristics of borosilicate clad fused silica core fiber optical waveguides, Appl. Phys. Lett. 26(4) (1975) pp. 185-187, https://doi.org/10.1063/1.88109.
[65] K.E. Chisholm, K. Sugden, I. Bennion, Effects of thermal annealing on Bragg fibre gratings in boron/germania co-doped fibre, Journal of Physics D: Applied Physics 31(1) (1998) pp. 61-64, https://doi.org/10.1088/0022-3727/31/1/009.
[66] Y.K. Cheong, W.Y. Chong, S.S. Chong, K.S. Lim, H. Ahmad, Regenerated Type-IIa Fibre Bragg Grating from a Ge-B codoped fibre via thermal activation, Opt. & Laser Tech. 62 (2014) pp. 69-72, https://doi.org/10.1016/j.optlastec.2014.01.007.
[67] L. Dong, W.F. Liu, Thermal decay of fiber Bragg gratings of positive and negative index changes formed at 193 nm in a boron-codoped germanosilicate fiber, Applied optics 36(31) (1997) pp. 8222-8226, https://doi.org/10.1364/AO.36.008222.
[68] F.J. Dutz, A. Heinrich, R. Bank, A.W. Koch, J. Roths, Fiber-Optic Multipoint Sensor System with Low Drift for the Long-Term Monitoring of High-Temperature Distributions in Chemical Reactors, Sensors (Basel) 19(24) (2019), https://doi.org/10.3390/s19245476.
[69] T. Chen, R. Chen, C. Jewart, B. Zhang, J. Canning, K. Cook, K.P. Chen, Thermally Regenerated Fiber Bragg-Grating in Twin-Air-Hole Microstructure Fiber for High Temperature Pressure Sensing, in: S.J. Mihailov, H.H. Du, G. Pickrell, A. Wang, A. Mendez, E. Udd (Eds.) Fiber Optic Sensors and Applications VIII, SPIE, 2011, pp. 802807-8, https://doi.org/10.1117/12.884994.
[70] G. Li, M. Liu, Y. Li, B.-O. Guan, Fabrication and sensing characteristics of the chemical composition grating sensor at high temperatures, Microwave and Optical Technology Letters 54(1) (2012) pp. 71-75, https://doi.org/10.1002/mop.26454.
[71] J. Kumar, O. Prakash, R. Mahakud, S.K. Agrawal, S.K. Dixit, S.V. Nakhe, J. Canning, Wavelength independent chemical sensing using etched thermally regenerated FBG, Sensors and Actuators B: Chemical 244 (2017) pp. 54-60, https://doi.org/10.1016/j.snb.2016.12.128.
[72] G. Laffont, R. Cotillard, N. Roussel, R. Desmarchelier, S. Rougeault, Temperature Resistant Fiber Bragg Gratings for On-Line and Structural Health Monitoring of the Next-Generation of Nuclear Reactors, Sensors (Basel) 18(6) (2018) p. 1791, https://doi.org/10.3390/s18061791.
[73] M. Celikin, D. Barba, B. Bastola, A. Ruediger, F. Rosei, Development of regenerated fiber Bragg grating sensors with long-term stability, Opt. Exp. 24(19) (2016) pp. 21897-21909, https://doi.org/10.1364/OE.24.021897.
[74] P. Biswas, S. Sharma, J. Canning, S. Bandyopadhyay, Regenerated Gratings Redefined, Photonics and Fiber Technology 2016 (ACOFT, BGPP, NP), Optical Society of America, Sydney, 2016, p. BTh3B.3, https://doi.org/10.1364/BGPP.2016.BTh3B.3.
[75] W. Vogel, Glass Chemistry, 2. Ed. ed., Springer, Berlin/Heidelberg, 1994, ISBN 978-3-642-78725-6.
[76] V. de Oliveira, C.C. de Moura, M.A. Vincenti, S. Libera, A. Polimadei, M. Caponero, R.M. Montereali, H.J. Kalinowski, Partial regeneration of Aluminum coated FBG along 450 days, in: H.J. Kalinowski, J.L. Fabris, W. Bock (Eds.) International Conference on Optical Fibre Sensors (OFS24), International Society for Optics and Photonics, Curitiba, 2015, pp. 963440-4, https://doi.org/10.1117/12.2193138.
[77] M. Lancry, K. Cook, B. Poumellec, J. Canning, Investigation of structural glass relaxation in regenerated fiber Bragg gratings, Nonlinear Photonics, Optical Society of America, Sydney, 2016, https://doi.org/10.1364/ACOFT.2016.JT4A.27.

[78] H. Hosono, J. Nishii, High photosensitivity and nanometer-scale phase separation in GeO_2-SiO_2 glass thin films, Optics letters 24(19) (1999) pp. 1352-1354, https://doi.org/10.1364/OL.24.001352.
[79] H.Z. Yang, M.C. Paul, S. Das, A. Dhar, X.G. Qiao, N.A.M. Nazal, K.-S. Lim, H. Ahmad, Regenerated grating produced in a multimaterial glass-based photosensitive fiber with an ultrahigh thermal regeneration ratio, Opt. Exp. 27(4) (2019) p. 4329, https://doi.org/10.1364/oe.27.004329.
[80] L.-Y. Shao, T. Wang, J. Canning, K. Cook, H.-Y. Tam, Bulk regeneration of optical fiber Bragg gratings, Applied optics 51(30) (2012) pp. 7165-7169, https://doi.org/10.1364/AO.51.007165.
[81] G. Li, B.-O. Guan, Improvement on reflectivity of chemical composition gratings at high temperatures, Microwave and Optical Technology Letters 53(5) (2011) pp. 963-966, https://doi.org/10.1002/mop.25953.
[82] X. Qiao, Y. Wang, H. Yang, L. Li, D. Su, T. Guo, K.-S. Lim, H. Ahmad, Ultra-high Temperature Chirped Fiber Bragg Grating through Thermal Activation, IEEE Phot. Tech. Lett. 27(12) (2015) pp. 1305-1308, https://doi.org/10.1109/LPT.2015.2421272.
[83] R. Cotillard, G. Laffont, P. Ferdinand, Regeneration of tilted fiber Bragg gratings, in: J.M. López-Higuera, J.D.C. Jones, M. López-Amo, J.L. Santos (Eds.) 23rd International Conference on Optical Fibre Sensors, SPIE, Santander, 2014, pp. 91572S-4, https://doi.org/10.1117/12.2059285.
[84] M. Kristensen, J. Russell, S. Gao, K. Cook, J. Canning, Improved Spectral Resolution of Long-Period Fiber Grating Sensors for Ultra-High Temperature Environments Using Narrow Interferences between Regenerated Gratings, Bragg Gratings, Photosensitivity, and Poling in Glass Waveguides (BGPP), Optical Society of America, Barcelona, 2014, p. BM4D.6, https://doi.org/10.1364/BGPP.2014.BM4D.6.
[85] W. Liu, K. Cook, J. Canning, Regenerated long period gratings (LPGs) in boron-codoped germanosilicate optical fibre, 5th APOS Conference, SPIE, 2015, pp. 96552T-4, https://doi.org/10.1117/12.2182942.
[86] I. Abe, V. de Oliveira, H.J. Kalinowski, J.L. Pinto, Regenerated Bragg gratings in high birefringence optical fibres, in: J. Santos, B. Culshaw, J.M. Lopez-Higuera, W.N. MacPherson (Eds.) 4th European Workshop on Optical Fibre Sensors,, SPIE, 2010, pp. 76531L-4, https://doi.org/10.1117/12.866324.
[87] E. Lindner, Erzeugung und Eigenschaften hoch-temperaturstabiler Faser-Bragg-Gitter, PhD thesis, Friedrich-Schiller-Universität, Jena, 2012.
[88] L. Polz, Regenerieren von Faser-Bragg-Gittern in polarisationserhaltenden optischen Fasern, PhD Thesis, Friedrich-Schiller-Universität, Jena, 2017, https://doi.org/10.22032/dbt.33878.
[89] S. Bandyopadhyay, J. Canning, M. Stevenson, K. Cook, Ultrahigh-temperature regenerated gratings in boron-codoped germanosilicate optical fiber using 193 nm, Optics letters 33(16) (2008) pp. 1917-1919, https://doi.org/10.1364/OL.33.001917.
[90] M.L. Aslund, J. Canning, M. Stevenson, K. Cook, Thermal stabilization of Type I fiber Bragg gratings for operation up to 600°C, Optics letters 35(4) (2010) pp. 586-588, https://doi.org/10.1364/OL.35.000586.
[91] D. Barrera, V. Finazzi, J. Villatoro, S. Sales, V. Pruneri, Packaged Optical Sensors Based on Regenerated Fiber Bragg Gratings for High Temperature Applications, IEEE Sensors J. 12(1) (2012) pp. 107-112, https://doi.org/10.1109/JSEN.2011.2122254.
[92] A. Bueno, K. Chah, D. Kinet, P. Mégret, C. Caucheteur, Hydrogen influence on regenerated FBGs produced by the phase mask technique with 266 nm femtosecond pulses, Bragg Gratings, Photosensitivity, and Poling in Glass Waveguides (BGPP), Optical Society of America, Barcelona, 2014, https://doi.org/10.1364/BGPP.2014.BW4D.3.
[93] E. Lindner, C. Chojetzki, S. Brückner, M. Becker, M. Rothhardt, J. Vlekken, H. Bartelt, Arrays of Regenerated Fiber Bragg Gratings in Non-Hydrogen-Loaded Photosensitive Fibers for High-Temperature Sensor Networks, Sensors 9(10) (2009) pp. 8377-8381, https://doi.org/10.3390/s91008377.
[94] R. Chen, A. Yan, M. Li, T. Chen, Q. Wang, J. Canning, K. Cook, K.P. Chen, Regenerated distributed Bragg reflector fiber lasers for high-temperature operation, Optics letters 38(14) (2013) pp. 2490-2492, https://doi.org/10.1364/OL.38.002490.
[95] R. Chen, A. Yan, Q. Wang, K.P. Chen, Fiber-optic flow sensors for high-temperature environment operation up to 800° C, Optics letters 39(13) (2014) pp. 3966-3969, https://doi.org/10.1364/OL.39.003966.
[96] M.-H. Lai, D.S. Gunawardena, K.-S. Lim, H.-Z. Yang, H. Ahmad, Observation of grating regeneration by direct CO_2 laser annealing, Opt. Exp. 23(1) (2015) pp. 452-463, https://doi.org/10.1364/OE.23.000452.
[97] M.-H. Lai, K.-S. Lim, M.R. Islam, D.S. Gunawardena, H.-Z. Yang, H. Ahmad, Effect of CO_2 Laser Annealing on Stress Applying Parts Contributing Toward Birefringence Modification in Regenerated Grating in Polarization Maintaining Fiber, IEEE Photon. J. 7(5) (2015) pp. 1-9, https://doi.org/10.1109/JPHOT.2015.2477496.
[98] H. Liu, H.Z. Yang, X. Qiao, M. Hu, Z. Feng, R. Wang, Q. Rong, D.S. Gunawardena, K.-S. Lim, H. Ahmad, Strain measurement at high temperature environment based on Fabry-Perot interferometer cascaded fiber regeneration grating, Sens.&Act. A: Phys. 248 (2016) pp. 199-205, https://doi.org/10.1016/j.sna.2016.07.028.
[99] C.A.F. Marques, V. de Oliveira, H.J. Kalinowski, R.N. Nogueira, Production of optical notch filters with fine parameter control using regenerated fiber Bragg gratings, Optics letters 37(10) (2012) pp. 1697-1699, https://doi.org/10.1364/OL.37.001697.
[100] L. Polz, B. Hopf, A. Jarsen, M. Eitzenberger, M. Lindner, H. Bartelt, J. Roths, Regenerated Bragg Gratings in Panda Fibers for Simultaneous Temperature and Force Measurements at High Temperatures, Journal of Lightwave Technology 34(19) (2016) pp. 4550-4556, https://doi.org/10.1109/jlt.2016.2530860.
[101] H.Z. Yang, X.G. Qiao, Y.P. Wang, M.M. Ali, M.-H. Lai, K.-S. Lim, H. Ahmad, In-Fiber Gratings for Simultaneous Monitoring Temperature and Strain in Ultrahigh Temperature, Photonics Technology Letters, IEEE 27(1) (2015) pp. 58-61, https://doi.org/10.1109/LPT.2014.2361768.
[102] B. Zhang, M. Kahrizi, High-Temperature Resistance Fiber Bragg Grating Temperature Sensor Fabrication, IEEE Sensors J. 7(4) (2007) pp. 586-591, https://doi.org/10.1109/JSEN.2007.891941.
[103] G. Laffont, R. Cotillard, P. Ferdinand, Multiplexed regenerated fiber Bragg gratings for high-temperature measurement, Meas. Sc. & Tech. 24(9) (2013) p. 094010, https://doi.org/10.1088/0957-0233/24/9/094010.
[104] S.S. Chong, W.Y. Chong, S.W. Harun, H. Ahmad, Regenerated fibre Bragg grating fabricated on high germanium concentration photosensitive fibre for sensing at high temperature, Opt. & Laser Tech. 44(4) (2012) pp. 821-824, https://doi.org/10.1016/j.optlastec.2011.11.024.
[105] A. Méndez, V.P. Wnuk, M. Fokine, Å. Claesson, L.-E. Nilsson, S. Ferguson, T. Graver, Packaging Process of Fiber Bragg Grating Strain Sensors for use in High- Temperature Applications, in: M.A. Marcus, B. Culshaw, J.P. Dakin (Eds.) Fiber Optic Sensor Technology and Applications IV, SPIE, 2005, pp. 60040E-7, https://doi.org/10.1117/12.629984.
[106] M.L. Aslund, J. Canning, A. Canagasabey, R.A. de Oliveira, Y. Liu, K. Cook, G. Peng, Mapping the thermal distribution within a silica preform tube using regenerated fibre Bragg gratings, Int. J. Heat & Mass Trans. 55(11-12) (2012) pp. 3288-3294, https://doi.org/10.1016/j.ijheatmasstransfer.2012.02.032.
[107] S. Gao, J. Canning, K. Cook, Ultra-high temperature chirped fiber Bragg gratings produced by gradient stretching of viscoelastic silica, Optics letters 38(24) (2013) pp. 5397-5400, https://doi.org/10.1364/OL.38.005397.
[108] Z. Ran, H. Bao, K. Cook, X. Wu, Y. Rao, J. Canning, Combined regenerated fibre Bragg gratings and Fabry-Perot etalons for dual strain and temperature sensing, International Conference on Optical Fibre Sensors (OFS24), International Society for Optics and Photonics, 2015, pp. 963459-4, https://doi.org/10.1117/12.2194860.
[109] P.S. Reddy, R.L.N.S. Prasad, D.S. Gupta, M.S. Shankar, K.S. Narayana, P. Kishore, Encapsulated fiber Bragg grating sensor for high temperature measurements, Optical Engineering 50(11) (2011) pp. 114401-6, https://doi.org/10.1117/1.3644534.

[110] L.-Y. Shao, J. Canning, T. Wang, K. Cook, H.-Y. Tam, Viscosity of silica optical fibres characterized using regenerated gratings, Acta Materialia 61(16) (2013) pp. 6071-6081, https://doi.org/10.1016/j.actamat.2013.06.049.
[111] Y. Tu, S.-T. Tu, Y.-H. Qi, Thermal characteristics of silver-recoated regenerated grating sensors for high-temperature sensing, in: Y. Liao, W. Jin, D.D. Sampson, R. Yamauchi, Y. Chung, K. Nakamura, Y. Rao (Eds.) OFS2012 22nd International Conference on Optical Fiber Sensor, SPIE, 2012, pp. 84215E-4, https://doi.org/10.1117/12.975266.
[112] T. Wang, L.-Y. Shao, J. Canning, K. Cook, Temperature and strain characterization of regenerated gratings, Optics letters 38(3) (2013) pp. 247-249, https://doi.org/10.1364/OL.38.000247.
[113] G.-Y. Li, B.-O. Guan, The strain response of chemical composition gratings at high temperatures, Meas. Sc. & Tech. 20(2) (2009) pp. 025204-4, https://doi.org/10.1088/0957-0233/20/2/025204.
[114] N. Alberto, H. José Kalinowski, V. Neto, R. Nogueira, Diamond-coated fiber Bragg grating through the hot filament chemical vapor process for chemical durability improvement, Applied optics 56(6) (2017) pp. 1603-1609, https://doi.org/10.1364/AO.56.001603.
[115] P. Rinaudo, B. Torres, I. Paya-Zaforteza, P.A. Calderon, S. Sales, Evaluation of new regenerated fiber Bragg grating high-temperature sensors in an ISO 834 fire test, Fire Safety Journal 71 (2015) pp. 332-339, https://doi.org/10.1016/j.firesaf.2014.11.02.
[116] F.J. Dutz, S. Boje, U. Orth, A.W. Koch, J. Roths, High-Temperature Profile Monitoring in Gas Turbine Exhaust-Gas Diffusors with 6-Point Fiber-Optic Sensor Array, Turbomachinery Propulsion and Power (submitted manuscript).
[117] H. Xia, D. Byrd, S. Dekate, B. Lee, High-Density Fiber Optical Sensor and Instrumentation for Gas Turbine Operation Condition Monitoring, Journal of Sensors (1) (2013) pp. 1-10, https://doi.org/10.1155/2013/206738.
[118] G. Heiberg, J. Skaar, M. Fokine, L. Arnberg, A new method for temperature measurement in solidifying aluminum alloys by use of optical fiber Bragg grating sensors, Trans. Am. Foundry Soc. 110(2-117) (2002) pp. 383-392.
[119] M. Lindner, E. Tunc, K. Weraneck, F. Heilmeier, W. Volk, M. Jakobi, A.W. Koch, J. Roths, Regenerated Bragg Grating Sensor Array for Temperature Measurements During an Aluminum Casting Process, IEEE Sensors J. 18(13) (2018) pp. 5352-5360, https://doi.org/10.1109/jsen.2018.2837164.
[120] A.F. Fernandez, B. Brichard, F. Berghmans, H.E. Rabii, M. Fokine, M. Popov, Chemical composition fiber gratings in a high mixed gamma neutron radiation field, IEEE Trans. Nuc. Sci. 53(3) (2006) pp. 1607-1613, https://doi.org/10.1109/TNS.2005.863273.
[121] M. Lindner, D. Bernard, F. Heilmeier, M. Jakobi, W. Volk, A.W. Koch, J. Roths, Transition from purely elastic to viscoelastic behavior of silica optical fibers at high temperatures characterized using regenerated Bragg gratings, Opt Express 28(5) (2020) pp. 7323-7340, https://doi.org/10.1364/OE.384402.
[122] R. Teschner, Glasfasern, Springer, Berlin/Heidelberg, 2013, ISBN 978-3-642-38328-1.
[123] S.M. Wiederhorn, S.W. Freiman, E.R. Fuller Jr., C.J. Simmons, Effects of water and other dielectrics on crack growth, Journal of Materials Science 17(12) (1982) pp. 3460-3478, https://doi.org/10.1007/BF00752191.
[124] P.J. Lezzi, E.E. Evke, E.M. Aaldenberg, M. Tomozawa, Surface Crystallization and Water Diffusion of Silica Glass Fibers: Causes of Mechanical Strength Degradation, J. Am. Ceram. Soc. 98(8) (2015) pp. 2411-2421, https://doi.org/10.1111/jace.13597.
[125] S. von Dosky, W. Ens, H. Grieb, M. Hilsendegen, H. Schorb, Optical Fiber Temperature Measurement for Process Industry, AMA Conferences, Nürnberg, 2013, pp. 578-582, https://doi.org/10.5162/sensor2013/D6.3.
[126] W. Xie, S. Meng, H. Jin, C. Du, L. Wang, T. Peng, F. Scarpa, S. Huo, Measurement of the high-temperature strain of UHTC materials using chemical composition gratings, Meas. Sc. & Tech. 27(5) (2016) p. 055101, https://doi.org/10.1088/0957-0233/27/5/055101.
[127] S. Sandlin, A. Hokkanen, Enbedding optical fibers in metal alloys, IEEE Instrumentation and Measurement Magazine 6(2) (2003) pp. 31-36, https://doi.org/10.1109/MIM.2003.1200281.
[128] Y. Tu, Y.-H. Qi, Fabrication and thermal characteristics of Ti-Ag-Ni coated regenerated grating sensors for high-temperature sensing, in: T.S. Tu, K.J. Peters, W. Ecke, T.E. Matikas (Eds.) SPIE Smart Structures and Materials + Nondestructive Evaluation and Health Monitoring, SPIE, 2013, pp. 869309-7, https://doi.org/10.1117/12.2012117.
[129] P. Zhang, H. Yang, Y. Wang, H. Liu, K.-S. Lim, D.S. Gunawardena, H. Ahmad, Strain measurement at temperatures up to 800°C using regenerated gratings produced in the highGe-doped and B/Ge co-doped fibers, Applied optics 56(22) (2017) pp. 6073-6078, https://doi.org/10.1364/AO.56.006073.
[130] O. Frazao, J.P. Carvalho, L.A. Ferreira, F.M. Araújo, J.L. Santos, Discrimination of strain and temperature using Bragg gratings in microstructured and standard optical fibres, Meas. Sc. & Tech. 16(10) (2005) p. 2109, https://doi.org/10.1088/0957-0233/16/10/028.